Studying the effect of Keap1 on innate immune signaling pathways in *Mycobacterium avium* infection

Master thesis in Molecular Medicine

Do Ngoc Phuc Chau

June 2013

Acknowledgement

This study was carried out at the Mycobacteria Research Group, Deparment of Cancer Reseaarch and Molecular Medicine in the Faculty of Medicine, Norwegian University of Science and Technology (NTNU), Trondheim, Norway. Financial support was from the Norwegian Research Council.

I want to deliver my gratitude to my supervisor, Dr. Trude Helen Flo. Without her, I could not start and complete my thesis. In my mind, she is the most pateint, active and careful supervisor that I have known. Even she is always busy with all her projects, deadlines and her family, she always had time for both me and Birendra. “I knew that you had to stay up late to review our thesis, while we were peacefully sleeping and waiting for your comments. I am very grateful for that.”. I also thank Jane Atesoh Awuh, now is Dr. Jane. She is a hardworking person and has a scientist-ability in her. From practical experiments to analyzing results, I learnt a lot from her. I want to say “Tusen takk” to Anne Marstad, our lab-technicianfor helping us a lot in all the stuffs and equiments in the lab. I also dedicated my thankfulness to all persons in our small project, in the Mycobacteria Research Group, and in the IKM laboratory. They make me know more about Norwegian people from meetings and parties that we had. And I have been very enjoyed studying and living here during last 2 years, especially during the thesis time, even it is very tough to me.

I specially thank you my close friend, Nam, who helped me a lot from the time before I came to Norway. He helped me in information of studying at NTNU, living in Norway, stuffs to bring here, place to buy things, hanging out during beautiful days and special events, accompanying me in many trips... I can say, a lot. He also the one who gave me comfort when I had the bad time in my life. He is just liked a big brother to me.

Above all, I dedicate my love to my parents. They always worry about me, even I am the biggest daughter and old enough to take care of myself. And to my siblings. I love you so much!

Abstract

The Mycobacterium species include pathogens causing serious diseases in mammals. *Mycobacterium avium* complex (MAC), while it has low virulence to normal people, it is a high potential pathogen causing TB-like disease in AIDS patients. Keap1 have studies by many researchers as a potential treatment in cancers. And its multi-binding property might give it an important role as a link between ROS, inflammation and autophagy. We knocked down the Keap1 in primary human monocyte-derived macrophages and investigated its role in immune response mechanism and killing of *M. avium* in human primary macrophages. Here, we found that not only IKKβ is under Keap1's effect, but also all IKK complex molecules and TBK1 are also affected by Keap1. This leads to the higher protein level of NF-*κ*B in Keap1 knockdown compared to control cells. Moreover, in autophagy, Keap1 has negative effect on accumulation of LC3B ii protein-related autophagy. Further investigation, we observed that Keap1 allows the growth of intracellular mycobacteria during 3 days of infection. Our study was done *in vitro* and limited to the macrophages only, in summary, it does not necessarily mean that the Keap1 gives disadvantage in controlling the *M. avium* infection. The role of Keap1 in the adaptive immune system should be studied to see clearly the effect of Keap1 in whole system.

Abbreviations

AIDS	acquired immunodeficiency syndrome
APC	antigen-presenting cell
Atg	autophagy-related gene
ATP	adenosine triphosphate
BAF-A1	bafalomycin A1
BALB/c mice	albino, laboratory-bred strain mice
Bcl-2	B-cell lymphoma
BIR	baculovirus inhibitor of apoptosis protein repeat
BTB	broad complex, tramtrack, bric-a-brac
CFU	colony-forming unit
CLR	C-type lectine receptor
CNC	cap'n'collar
CTR	C-terminal Kelch domain
Cul3	Cullin 3
CytC	cytochrome C
DAI	DNA-dependent activator of IRFs
DAMP	damage-associated molecular pattern
DC-SIGN	dendritic cell-specific intercellular adhesion molecules-3 grabbing nonintegrin
DGR	double glycine repeat
dsRNA	double-stranded RNA
ELISA	enzyme-linked immunosorbent assay
ERK	extracellular signal-regulated kinase
GAPDH	glyceraldehyde 3-phosphate dehydrogenase
GM-CSF	granulocyte-macrophage colony-stimulating factor
Gst	glutathione S-transferase
GTP	guanosine triphosphate
HIV	human immune-deficiency virus infection
HRP	horseradish peroxidase
HSP	heat-shock protein
IFN	interferon
IKK	I*κ*Bα kinase
IL	interleukin
iNOS	inducible nitric oxide synthase
INrf2	inhibitor Nrf2
IRAK	IL-1R-associated kinase
IRF	interferon regulatory factor
IVR	intervening region
I*κ*Bα	inhibitor *κ*B-α
JNK	c-Jun N-terminal kinase
Keap1	Kelch-like ECH-associated protein 1
KIR	Keap1-interaction region
LAM	lipoarabinomannan
LC3	light chain 3
LIR	LC3-interacting region
LM	lipomannan
LRR	leucine-rich repeat
LT	lymphotoxin
M. avium	*Mycobacterium avium*
M. tb	*Mycobacterium tuberculosis*
MAC	*Mycobacterium avium* complex
MAL	MyD88 adaptor-like
ManLAM	mannose-capped LAM
MAPK	mitogen activated protein kinase
MD2	myeloid differentiation 2
MDM	monocyte-derived macrophage
MEK	mitogen-activated protein kinase
MHC	major histocompatibility complex

MOI	multiple of infection
MPTP	1-methyl-4-phenyl-1,2,3,6-tetrahydropyridine
mTOR	mammalian target rapamycin
MyD88	myeloid fifferentiation primary-response protein 88
NBR1	neighbor of BRCA1 gene 1 protein
NF-κB	nuclear factor κB
NLR	NOD-like receptor
NOD	nucleotide-binding oligomerization domain
Nqo1	NAD(P)H dehydrogenase, quinone 1
Nrf2	nuclear factor- erythroid 2-related factor 2
PAMP	pathogen-associated molecular pattern
PB1	Phox and Bem1p
PBMC	peripheral blood mononuclear cell
PI3K	phosphoinositide 3-kinase
PIM	phosphatidyl-inositol mannoside
PKC	protein kinase C
POZ	poxvirus, zinc finger
PRR	pattern recognition receptor
PTGS	post-transcriptional gene silencing
PVDF	polyvinylidene flouride
qPCR	quantitative polymerase chain reaction
Rbx1	RING-box protein1
Rg	rough
RIG	retinoic acid-inducible gene
RIP1	ribosome inactivating protein 1
RISC	RNA-induced silencing complex
RLR	RIG-like receptor
RNAi	RNA interference
ROS	reactive oxygen species
RT-PCR	real-time polymerase chain reaction
SDS-PAGE	sodium dodecyl sulfate polyacrylamide gel electrophoresis
SEM	standard error of the mean
siRNA	small interfering RNA
SmO	smooth opaque
SmT	smooth transparent
SQSTM1	Sequestosome 1
STAT1	signal transducers and activators of transcription 1
STING	stimulator of interferon gene
TB	tuberculosis
TBK1	TANK-binding kinase 1
TICAM-1	TIR-domain-containing adapter molecule 1
TIR	Toll-interleukin 1 receptor
TIRAP	TIR-domain-containing adapter protein
TLR	Toll-like receptor
TNF	tumor necrosis factor
TRAF-6	TNF-receptor-associated factor 6
TRAM	TRIF-related adapter molecule
TRIF	TIR-domain-containing adapter-inducing interferon-β
Ub	ubiquitin
UBA	ubiquitin associated domain
UNG	uracil-N-glycosylase
VDAC	voltage-dependent anion channel
WHO	World Health Organization
ZZ	zinc finger

List of figures

Figure 1.1: Colony morphology of *M. avium* 104 2

Figure 1.2: Cellular trafficking pathway within mycobacteria-infected macrophage 4

Figure 1.3: Signaling molecules of pattern recognition receptors 6

Figure 1.4: The classical NF-□B signaling pathway.....9

Figure 1.5: TLR-mediated IRF activation pathways in specific cell types.....10

Figure 1.6: Overview of activation and inactivation of Nrf2 signaling pathway 12

Figure 1.7: Molecular signaling in autophagy 14

Figure 1.8: Structure of Keap1 (or INrf2).....15

Figure 1.9: Mechanism of Keap1 as interplay factor of oxidative stress, autophagy and inflammatory.....16

Figure 1.10: Interaction between Beclin-1 and Bcl-2 affects autophagy.....18

Figure 1.11: Schematic model of Keap1 regulating Bcl-2 family 19

Figure 1.12: Structure of multidomain p62 protein 20

Figure 3.1: Principle of siRNA transfection. 24

Figure 3.2: Mechanism of action of bafilomycin A1 (BAF-A1) in autophagy 26

Figure 3.3: Basic principles of the western blotting 27

Figure 3.4: Basic procedure of western blotting.....27

Figure 3.5: Action of TaqMan probe with reporter and quencher.....32

Figure 4.1: Time of infection affects the phosphorylation of inflammatory signaling proteins in M. avium infected MDMs.....36

Figure 4.2: Level of Keap1 in siRNA knockdown compared to siNTC sample 37

Figure 4.3: One representative western-blot used to quantify level of proteins in three different inflammatory pathways.....37

Figure 4.4: Keap1 down regulated the NF-□B signaling pathway through IKK complex during M. avium infection.....39

Figure 4.5: Keap1 regulates TBK1 protein in type I IFN signaling pathway during M. avium infection 40

Figure 4.6: Keap1 had no effect on p38-MAPK protein during M. avium infection).....41

Figure 4.7: M. avium infection induces autophagy in primary human macrophage 42

Figure 4.8: One representive western-blot used to quantify Keap1 and LC3B protein.....43

Figure 4.9: Effect of Keap1 on LC3B ii induction by immuno-blot method 44

Figure 4.10: Effect of Keap1 on LC3B ii induction by confocal microscopy method.....45

Figure 4.11: The growth of intracellular M. avium might be affected by Keap1 46

Figure 4.12: Screening for the detected amount of human and mycobacterial cells by duplex PCR 47

Figure 4.13: Mycobacterial cells in infected human macrophages as measured by colony counting (CFU) and qPCR (PCR).....48

List of tables

Table 3.1. Keap1 siRNA sequences.....25

Table 3.2. Primary and secondary antibodies for protein assessment by western blotting. (*) is the secondary antibody 30

Table 3.3: Sequences' information of primers and probes used in duplex real-time qPCR.....32

Table 3.4: Estimated amount of sterile water for different types of plate to get appropriated amount of cell solution for bead-beating 33

Table 3.5: Volume per reaction mixture for qPCR.....34

Table of content

1. Introduction 1

1.1 Mycobacterial infections 1

1.1.1 Mycobacterium avium complex 1

1.1.2 Infection mechanism 2

1.2 Innate immune defense system against mycobacterial infection 4

1.2.1 Humoral immune responses 4

1.2.2 Reactive oxygen species 11

1.2.3 Autophagy 13

1.3 *Keap1* – the interplay factor in the innate immune system 15

1.3.1 Structure of Keap1 15

1.3.2 Keap1 and Nrf2 in ROS 16

1.3.3 Keap1 and IKKβ in inflammatory pathway 17

1.3.4 Keap1 and Bcl-2 and p62 in autophagy 17

2. Aim and objectives 21

3. Methodology 22

3.1 Cells 22

3.2 Mycobacterial culture 23

3.3 *Keap1* siRNA transfection assay 23

3.4 *In vitro* infection and time-course experiments 25

3.5 Western blotting 26

3.5.1 Basic principles 26

3.5.2 Standard procedures 27

3.5.3 Approaches for good western blotting.....29

3.5.4 Antibodies 30

3.6 Optimize the protocol for multiplex real-time Polymerase Chain Reaction (RT-PCR) to quantify Mycobacterial cells per human cell 31

3.6.1 Basic principles 31

3.6.2 Procedure 32

3.7 Statistical analysis 34

4. Results 35

4.1 Keap1 negatively regulates inflammatory signaling in *M. avium* infected primary human macrophages..... 35

4.1.1 Kinetics of phospho-(p-)IKKα/β and p-NF-κB proteins produced in M. avium infected MDMs 35

4.1.2 Keap1 down regulated the NF-κB signaling pathway through IKK complex during M. avium infection 36

4.1.3 Keap1 negative regulates TBK1 during M. avium infection 40

4.1.4 Keap1 has no effect on p38 in MAPK pathway.....41

4.2 Keap1 down regulated the autophagy LC3B ii protein in MDMs..... 41

4.3 Keap1 affects the survival of intracellular *M. avium* in MDMs 45

4.4 Quantitation of Mycobaterial cells per human cell by PCR 46

5. Discussion.....49

6. Conclusions and future perspectives.....54

References.....55

1. Introduction

1.1 Mycobacterial infections

The Mycobacterium species include pathogens causing serious diseases in mammals. One of them is tuberculosis (TB), a contagious disease caused by a single infectious agent spreading through the air. It is second only to human immune-deficiency virus infection / acquired immunodeficiency syndrome (HIV/AIDS) as the greatest killer worldwide and occurs in every part of the world, especially Africa and Asia. According to the report of World Health Organization (WHO) in 2011, about 8.7 million people fell ill with TB, 1.4 million people died from TB, and 10 million children were orphaned as the result of their parents' death from TB (centre, 2013). Most TB-infected patients got infection from *Mycobacterium tuberculosis* (*M. tb*). Commonly, AIDS patients who are with TB-like disease or who easily get TB development have infection of *Mycobacterium avium* complex (MAC), while it has low virulence to normal people. In addition, *Mycobacterium africanum* infection can cause TB-like symptoms with lower pathogenicity. Other diseases caused by Mycobacterial species can be counted, including bovine TB, leprosy etc. (Wolinsky, 1992)

1.1.1 Mycobacterium avium complex

Mycobacterium is a genus of Actinobacteria growing in the mold-like fashion on the surface of cultured liquids. Mycobacteria are considered as Gram-positive, aerobic and non-motile bacteria with acid-alcohol-fast characteristics. Their cell wall is characteristically thick, hydrophobic, waxy and rich in mycolic acids or mycolates, having an important role in the natural resistance to antibiotics (Jarlier & Nikaido, 1994). It consists of the hydrophobic mycolate layer and a peptidoglycan layer containing *N*-glycolylmuramic acid held together by a polysaccharide, arabinogalactan. With the outer layer composed of free lipids, proteins and lipoglycans; and the interspersed layer composed of phosphatidyl-inositol mannosides (PIMs), lipomannan (LM) and lipoarabinomannan (LAM), the cell wall makes a substantial contribution to the hardiness of this genus (Brennan, 2003). The mycobacterial cells are straight or slightly curved rods with 0.2 to 0.6μm in width and 1 to 10μm in length (*Sherris Medical Microbiology*, 2004). Some species are difficult to culture with long reproductive cycles. Therefore, a natural division was made between slowly- and

rapidly-growing species. In medical classification, they are divided into several groups based on the pathogenicity and places of living or residing for purpose of diagnosis and treatment.

Mycobacterium avium-intracellular complex (MAC) is a family of genetically related bacteria, including *Mycobacterium avium* (*M. avium*) and *Mycobacterium intracellulare*. These atypical mycobacteria are widely distributed in nature, such as in water, soil, unpasteurized milk, and animals. *M. avium* is considered an opportunistic mycobacterium causing non-tuberculous pulmonary disease in the later stages of AIDS, in immuno-compromised people, genetic-deficiency individuals, healthy children, in some elderly men and women with Lady-Windermere syndrome (Koirala, 2012). When people inhale or swallow contaminated aerosol, food or water, MAC bacteria will cause infection with symptoms reminiscent of tuberculosis. Cervical lymphadenitis is also found in non-tuberculous *M. avium* infection in children, who do not develop pulmonary diseases (C. Bryan, 2011).

The MAC has variable virulence with different morphology and strain. From 1970, many studies have shown a correlation between the morphology and virulence of mycobacteria. In one study, Pedrosa and others infected albino, laboratory-bred strain (BALB/c) mice with environmental MAC. They found that smooth transparent (SmT) colonies on solid media were virulent and caused progressive infection, in contrast, smooth opaque (SmO) colonies were avirulent and were eliminated slowly from infected organs, while rough (Rg) colonies showed either virulence or avirulence (Pedrosa et al., 1994). Also in their study, they proved the virulent property of MAC isolated from infected humans in BALB/c mice. In addition, Torrelles and others used the expression of glycopeptidolypid to show the same virulent characteristics of *M. avium* strain 104 on mice for all phenotypes of SmO, SmT and Rg colonies (figure 1.1) (Torrelles et al., 2002).

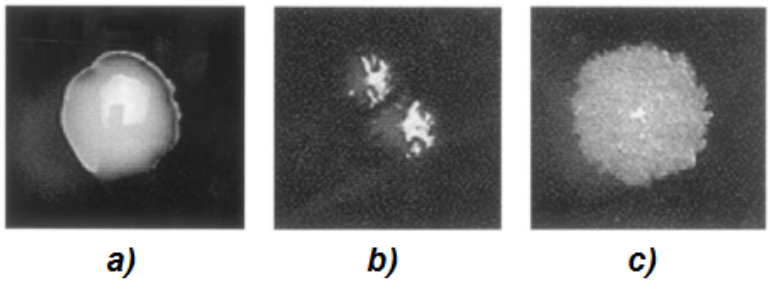

Figure 1.1: Colony morphology of *M. avium* 104. a) Smooth opaque (SmO) morphotype is avirulent, b) smooth transparent (SmT) colonies are virulent, and c) rough (Rg) morphotype is either avirulent or virulent. (taken from Torrelles *et al.*, 2002)

1.1.2 Infection mechanism

Although different mycobacteria have different routes of infection, the pathogenic mycobacteria occupy the same characteristics of evading the elimination of cell-mediated immune response (Appelberg, 2006). Mycobacteria have a general mechanism of action when they reach the

lungs and are phagocytosed by macrophages, like other bacteria or pathogens. When mycobacteria are phagocytosed by the macrophages, the macrophages will produce pro-inflammatory responses that attract other immune cells, such as monocytes, macrophages, neutrophils and dendritic cells to the site of infection for immunity responses. The responses are initiated by the process that the macrophages will take an action to destroy the pathogens and present the patterns for immune system by major histocompatibility complex (MHC). This process is called phagolysosome maturation (Aderem & Underhill, 1999).

However, mycobacterium has developed mechanisms that prevent the phagolysosomal fusion for evading elimination of cell-mediated immune response (figure 1.2). By arresting early endosomal stage of mycobacterial phagosome, they can avoid the killing and reside successfully in macrophages (Aderem & Underhill, 1999; Flynn & Chan, 2001). In *M. tb* infection, when the early innate immune responses recruit other immune cells to the site of infection, the invading *M. tb* eventually infect to those cells and increase the population leading to the formation of granuloma (Davis & Ramakrishnan, 2008). This granuloma provides a cellular niche for mycobacterial replication. Every organism depends on iron for growing. Mycobacteria residing in phagosomes have an ability to produce mycobactin sidephores for scavenging iron from endocytosed transferrin or intracellular iron stores within the host system (Halaas et al., 2010; Holmes, Paulsene, Jide, Ratledge, & Strong, 2005; Ratledge, 2004). The produced sidephores in two major forms are cell-wall associated mycobactins and water-soluble carboxymycobactins. When the immune system is weakened by factors, such as drug therapy or co-infection with HIV, the granuloma loses its solidity and starts to decay from the center. Then, there is the chance for dormant mycobacteria to wake up, replicate rapidly and spread to other tissues and/or organs through blood stream.

Thus, by preventing the phagolysosomal maturation, mycobacteria can avoid the antimicrobial environment outside the cell initiated by the innate immune system, prevent the antigen processing and presentation for the activation of the adaptive immunity, and access to the host-derived irons for survival and growing.

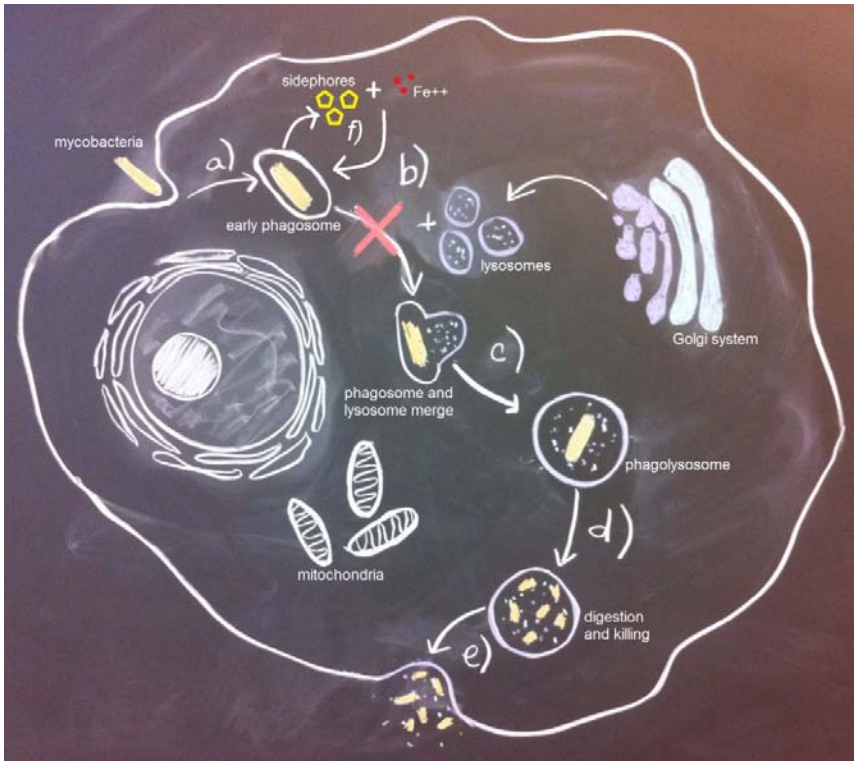

Figure 1.2: Cellular trafficking pathway within mycobacteria-infected macrophage. a) The mycobacteria is engulfed by macrophage forming early phagosome within the macrophage. Normally, phagosome proceeds to merge with lysosome formed from the Golgi system at stage b). However, the mycobacteria has ability to block the whole process from this stage, preventing lysosome fusion, inhibiting (c) phagolysosome maturation, and (d) pathogen-digesting and killing by lysosome enzymes for (e) defecating outside the cell. Moreover, the resided mycobacteria can produce sidephores to sequester iron within the cell for its growth and survive (f).

1.2 Innate immune defense system against mycobacterial infection

The human body is protected from outside pathogenic microorganisms and cancer by a remarkably versatile defense system, the immune system. The meaning of immunity comes from the Latin term *immunis*, meaning "exempt", the state of protection from infectious diseases (Goldsby, Kindt, & Osborne, 2000). This biological system involves the structures and processes within an organism that protect against disease, the generation of an enormous numbers of cells and molecules acting together in a dynamic network that specifically recognizes and eliminates an apparently limitless variety of foreign invaders. This system protects the host with layer-defenses of increasing specificity: the primitive innate immunity barriers and the specific adaptive immunity responses. The innate immune system is the first line of host defense and also important for the activation of acquired immunity.

1.2.1 Humoral immune responses

Innate immune system is constituted of cells such as neutrophils, macrophages, dendritic cells, natural killer cells, eosinophils, basophils and mast cells; and is activated by germline-encoded

receptors on the surface of cells called pattern recognition receptors (PRRs). The PRRs are responsible for sensing the presence of invading microorganisms and damaged cells by recognizing pathogen-associated molecular patterns (PAMPs) and damage-associated molecular patterns (DAMPs). Five different classes of PRR families have been identified: Toll-like receptors (TLRs), Retinoic acid-inducible gene (RIG)-I-like receptors (RLRs), Nucleotide-binding oligomerization domain (NOD)-like receptors (NLRs), C-type lectin receptors (CLRs), and DNA sensors (Kumar, Kawai, & Akira, 2011; Takeuchi & Akira, 2010). They have different cellular locations that are able to respond to both extracellular and intracellular microbes. Activation of PRRs is a complex downstream signaling event leading to the secretion of various inflammatory cytokines, chemokines, and antimicrobial proteins (figure 1.3). This will result in activating the first defense line of antigen-presenting cells (APCs), production of pro-inflammatory cytokines, type 1 interferons (IFN) and chemokines, promoting the phagocytosis to engulf and digest the pathogens, and the expression of the peptide antigen on the cell surface, and influencing as a bridge to activate adaptive immune response by activating T-cells and B-cells (Barton & Medzhitov, 2003; Kawai & Akira, 2006; Kiyoshi & Shizuo, 2004).

TLRs

The TLR family is one of the most important and the best characterized of the PRR families and plays a critical role in recognizing the broadly shared PAMPs from invading pathogens outside of the cell and in intracellular endosomes and lysosomes. The TLRs, were first discovered in Drosophila as toll proteins, and are single, membrane-spanning, non-catalytic receptors. They are characterized by the N-terminal leucine-rich repeats (LRRs) and transmembrane region of a cytoplasmic Toll-interleukin 1 receptor homology (TIR) domain. Ten TLRs have been found in human cells recognizing molecules that are constantly associated with threats and are highly specific to these threats. Because TLRs are specific, they can not easily be changed during the evolution (Janssens & Beyaert, 2003).The TLRs are located on the cell surface or intracellular membrane of many cell types and recognize a wide range of pathogenic endogenous and exogenous ligands (appendix 1: TLR-family members, their ligands and origin, and their distribution in human cells). When TLRs are activated, one or more of four adapter molecules within the cytoplasm of cells, known as myeloid differentiation primary-response protein 88 (MyD88), TIR-domain-containing adapter protein (TIRAP) or MyD88 adaptor-like (MAL), TIR-domain-containing adapter-inducing interferon-β (TRIF) or TIR-domain-containing adapter molecule 1 (TICAM-1) and TRIF-related adapter molecule (TRAM), will be recruited and activate other molecules within the cell (Kawai & Akira,

2011; Kumar et al., 2011; Takeuchi & Akira, 2010). Different TLRs can initiate different and independent, but overlapping, sets of biological effects, and contribute to both common and unique aspects of signaling mechanisms (Kawai & Akira, 2011).

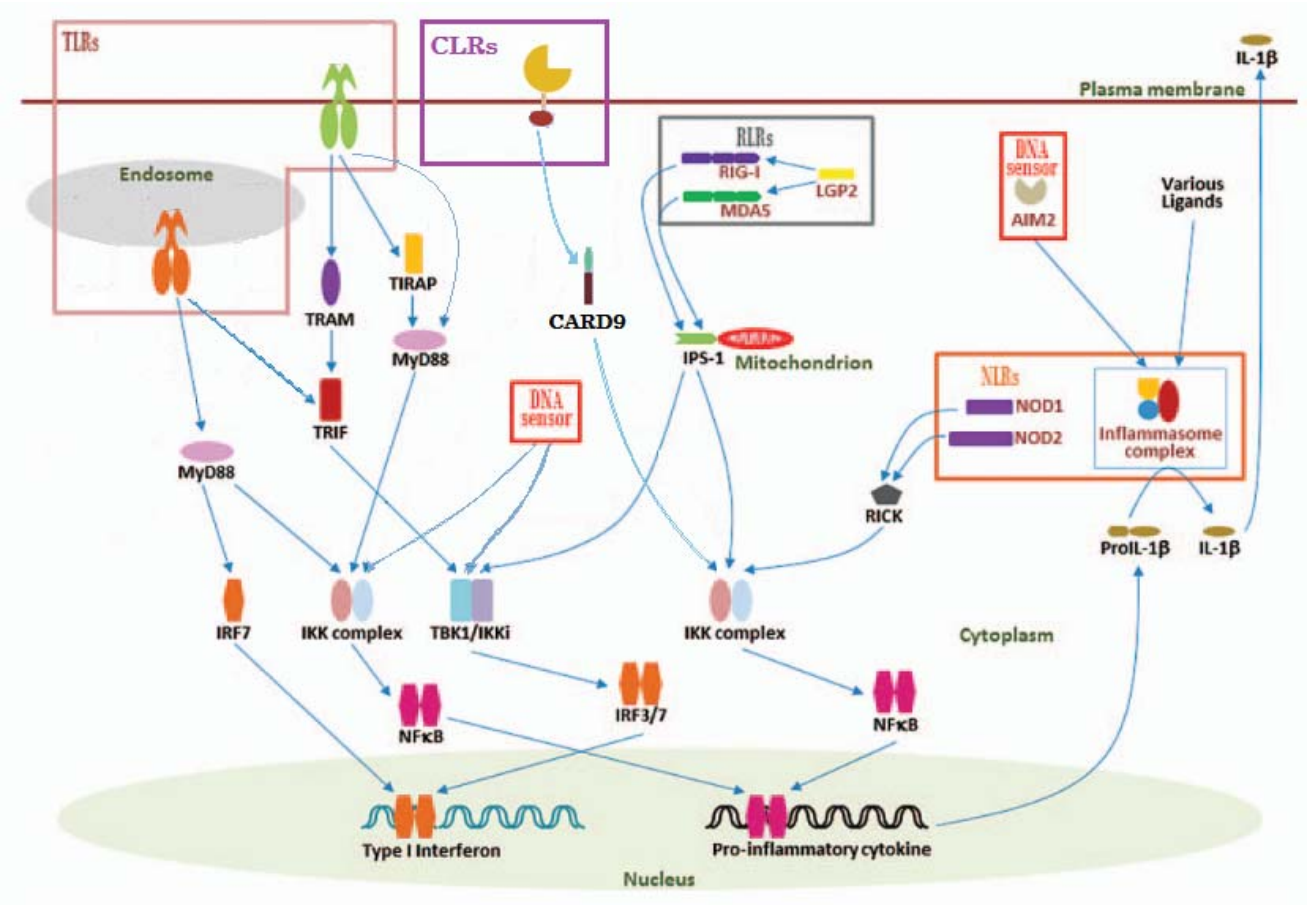

Figure 1.3: Signaling molecules of pattern recognition receptors. PRRs include the Toll-like receptors (TLRs), Retinoic acid-inducible gene (RIG)-I-like receptors (RLRs), Nucleotide-binding oligomerization domain (NOD)-like receptors (NLRs), C-type lectin receptors (CLRs) and DNA sensors. TLRs are located on the cell membrane and in the endosomes. RLRs, NLRs and other sensors are in the cytosol, while CLRs mainly are transmembrane receptors. These receptors are initiated differently and independently for sets of cross-talk biological effects with two main outcomes. One is nuclear factor-κB (NF-κB), which is activated by most of PRRs, leading to the transcription of proinflammatory cytokines, which are activated by inflammasome complex. And, the other is interferon regulatory factor (IRF) activated by the RLRs, some TLRs, which results in the production of type I interferons. Taken and modified from (de Koning, Simon, Zeeuwen, & Schalkwijk, 2012; Kumar et al., 2011)

Many studies have reported that mycobacterial recognition by TLRs includes TLR2 together with TLR1 or TLR6, complex of TLR4 with other molecule known as myeloid differentiation 2 (MD2), and TLR9 (Bulut et al., 2005; Kleinnijenhuis, Oosting, Joosten, Netea, & Crevel, 2011; Manzanillo, Shiloh, Portnoy, & Cox, 2012). While TLR2 together with TLR1 and TLR6 can

recognizes variety of mycobacterial cell wall antigens such as LAM, LM, PIM, triacylated lipoprotein and diacylated lipoprotein, TLR4 can be activated by mycobacteria-secreted heat shock protein, and TLR9 recognizes mycobacterial DNAs which are escaped from arrested phagosomes to the cytosol. Recently it was also found that, TLR8 has four polymorphisms associated with TB susceptibility in males (Davila et al., 2008). All these TLRs recruit MyD88 to the TIR domain and initiate MyD88-dependent signaling pathway. The downstream outcome of this pathway is the activation of nuclear factor-κB (NF-κB), a transcription factor, and mitogen activated protein (MAP) kinases (MAPKs) to activate many pro-inflammatory genes inducing cytokines, chemokines, proteins of the complement system, enzymes, adhesion molecules, and immune receptors. Moreover, TLR4 utilizes another so-called MyD88-independent pathway through the TRAM molecule. The result of this signaling pathway is the activation of either transcription factor NF-κB or interferon (IFN) regulatory factor (IRF) 3 or 7, which are very important in expression of type I IFN genes for antimicrobial activities. This pathway can also activate the second phase of NFκB and MAPK activation for inflammatory cytokine induction (Kagan et al., 2008).

RLRs, CLRs, NLRs, inflammasomes and DNA sensors

The RLRs include three members: RIG-I and MDA5 are essential for recognition of various RNA from RNA viruses in the cytoplasm of infected cell, and LGP2 is responsible for negative or positive regulation depending on the type of RNA viruses. These RLRs once triggered will induce various antiviral and inflammatory responses. *M. tb* has a special ESX-1 secreted system to permeabilize phagosomal membrane (Abdallah et al., 2007). This allows mycobacterial proteins and DNAs going to the host cytosol, and the mycobacterial DNA can be recognized by different cytosolic DNA receptors. STING (stimulator of interferon genes) is one of the adaptors involved in the RLR signaling pathway. In many cell types, when coupled with a cytosolic DNA sensor, STING triggers the type-I IFN response via TANK-binding kinase 1 (TBK1) and suppresses viral replication (Kawai & Akira, 2006; Kumar et al., 2011). Different levels of response depend on the different forms of structural DNA (Kawai & Akira, 2009).

There are at least five subfamilies of NLRs responsible for detecting PAMP and endogenous molecules in cellular cytosol: NLRA containing an acidic transactivation domain, NLRB containing a baculovirus inhibitor of apoptosis protein repeat (BIR), NLRC containing a CARD domain, NLRP containing a purin domain and NLRX with an unknown domain. NOD1 and NOD2 are two well-studied NLRs and mainly expressed in the cytosol (Kufer, Kremmer, Adam, Philpott, & Sansonetti,

2008). They are responsible for induction of inflammatory cytokines, which are forms of cell death, pyroptosis and pyronecrosis, and other antimicrobial genes production such as tumor necrosis factor (TNF)-α, IFN-γ, and interleukin (IL)-1 family cytokines (Franchi, Warner, Viani, & Nunez, 2008; Kawai & Akira, 2009; Lavelle, Murphy, O' Neill, & Creagh, 2009). Some NLRs form a large intracellular complex that is referred to as the "inflammasome" in cytosols (Ishii, Koyama, Nakagawa, Coban, & Akira, 2008; Martinon, 2010). They involve NALP3, NALP4 and IPAF, where the NALP3 inflammasome is the most widely studied inflammasome. This protein complex will associate with pro-caspase-1 and promote the proteolytic cleavage to yield caspase-1 for the activation of IL-1 and IL-18 from pro-IL-1 and pro-IL-18, respectively. In their studies, Gandotra *et al.* showed the participation of NOD2 in macrophages and dendritic cells from *M. tb*-infected mice (Gandotra, Jang, Murray, Salgame, & Ehrt, 2007). However, although the NOD2-deficient mice showed the reduced production of proinflammatory cytokines and nitric oxide, the susceptibility of *M. tb* infection was no difference compared to wild-type mice.

Another important PRR class is CLRs, the transmembrane receptors characterized by the presence of a carbohydrate-binding domain. Many studies have shown a dual function of CLRs and their signaling will shape the immune responses (Cambi & Figdor, 2003; Geijtenbeek & Gringhuis, 2009). CLRs can either stimulate the production of inflammatory cytokines or inhibit the TLR-mediated immune complexes (Takeuchi & Akira, 2010). Their signaling pathways are initiated via ITAM domain or adaptor harboring an ITAM domain, such as FcRγ, DAP10 or DAP12, for activation of MAP kinases, transcription factor NF-AT and NF-κB. Mycobacterial cell wall consists of mannose-capped lipoarbinomannan (ManLAM) and LM which can be recognized by CLRs, such as mannose receptors, dectin-1 and dendritic cell-specific intercellular adhesion molecules-3 grabbing nonintegrin (DC-SIGN) (Geijtenbeek et al., 2000). The activation will lead to the production of anti-inflammatory cytokines and reduces the activation of oxidative stress responses.

The NF-κB signaling pathway

The transcription factor NF-κB is a central inflammatory mediator of the immune system. There are two NF-κB signaling pathways: the classical pathway which is mostly involved in innate immunity and the alternative pathway which may be involved in adaptive immunity. The classical NF-κB pathway is activated by different PRRs and dependent on the phosphorylation of IκB through inhibitor κB (IκB)-α kinase (IKK) complex, especially IKKβ and IKKγ. The alternative NF-κB

pathway is not dependent on IKKβ but is strictly dependent on IKKα; it is activated through members of the TNF cytokines family but not by TNF-α (Ramakrishnan, Wang, & Wallach, 2004).

The classical pathway is the most well-studied in NF-κB signaling through PRRs (figure 1.4). Upon the appropriate activation, the TLRs form dimers and recruit adaptor molecules like MyD88. The interacted TIR/MyD88 domain recruits the IL-1R-associated kinase (IRAK), a serine/threonine kinase through death domain to MyD88. The IRAK-4 and IRAK-1 form a complex that recruits, phosphorylates and activates the TNF-receptor-associated factor 6 (TRAF-6) when it is dissociated from MyD88. The IRAK-1/TRAF-6 complex which in turn will activates downstream kinases, which are capable of activating the IKK complex. The activation of IKKβ of IKK complex will lead to the phosphorylation and degradation of IκB releasing free NF-κB (dimer of p50 and p65). In the absence of stimuli, the NF-κB is held in cytoplasm by inhibitory IκB protein. Free NF-κB is active, translocates to nuclear and initiates the transcription of target genes (Kawai & Akira, 2006).

The NF-κB regulates the expression of a wide variety of critical genes in innate immune responses. Reviewed by Hayden and Ghosh, they include many cytokines (such as IL-1, IL-2, IL-6, IL-12, TNF-α, lymphotoxin (LT) α, LTβ and granulocyte-macrophage colony-stimulating factor (GM-CSF)), adhesion molecules (such as intercellular adhesion molecule, vascular cell adhesion molecule, and endothelial leukocyte adhesion molecule), chemokines (such as IL-8), acute phase proteins (Hayden & Ghosh, 2011), and inducible enzymes and protaglandins (such as inducible nitric oxide synthetase and cyclooxygenase 2)(Catley, Chivers, & Cambridge, 2003; Farlik et al., 2010; Poligone & Baldwin, 2001), as well as some antimicrobial peptides (such as defensins, lipocalin 2) (Ayabe et al., 2000; Flo et al., 2004).

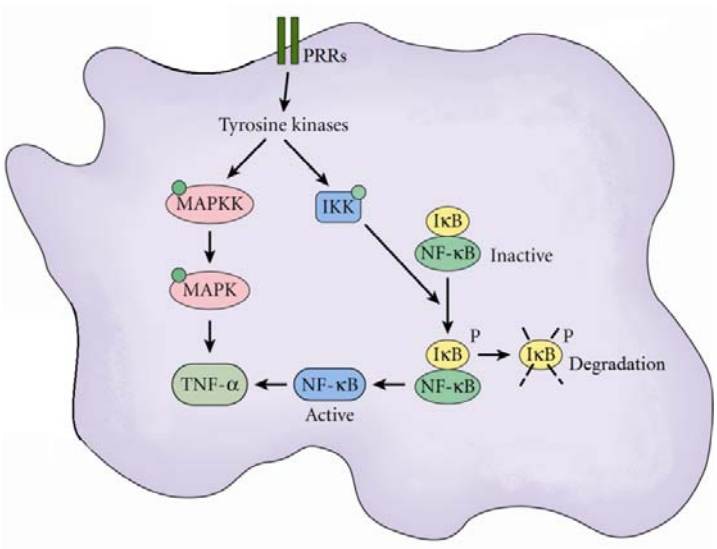

Figure 1.4: The classical NF-κB signaling pathway. Activation of PRRs recruits adaptor molecules like MyD88 that in turn will activate downstream kinases that are capable of activating the IKK complex. The activation of IKKβ of IKK complex will lead to the phosphorylation and degradation of IκB releasing free NF-κB. Free NF-κB is active, translocates to nucleus and initiates the transcription of target genes such as TNF-α. In addition, the MAPK pathway is also activated downstream of PRRs through a series of phosphorylation and affects TNF-α production.

The Interferon (IFN) signaling pathway

Recently, more and more evidence provides insight to the role of IFN in viral interference (Kumar et al., 2011). The IFNs are widely expressed cytokines with strong antiviral properties, but are also involved in the response to bacterial ligands and inflammasomes. In humans, the IFNs are classified into three main groups. The type I IFN family includes IFN-α subtype, IFN-β, IFN-ε, IFN-κ and IFN-ω. The IFN-γ is the only cytokine belonged to the type II IFN having both antibacterial and antiviral activities. The type III IFN consists of IFN-λ1 (IL-29), IFN-λ2 (IL-28A) and IFN-λ3 (IL-28B) (Pestka, Krause, & Walter, 2004). The induction of type I IFN depends on the cell types and ligands. IRF3, IRF5 and IRF7 are members in the IRF family of transcription factors having a crucial role in the type I IFN expression and playing a direct role in microbe-induced signaling (Honda & Taniguchi, 2006; Tamura, Yanai, Savitsky, & Taniguchi, 2008; Taniguchi, Ogasawara, Takaoka, & Tanaka, 2001).

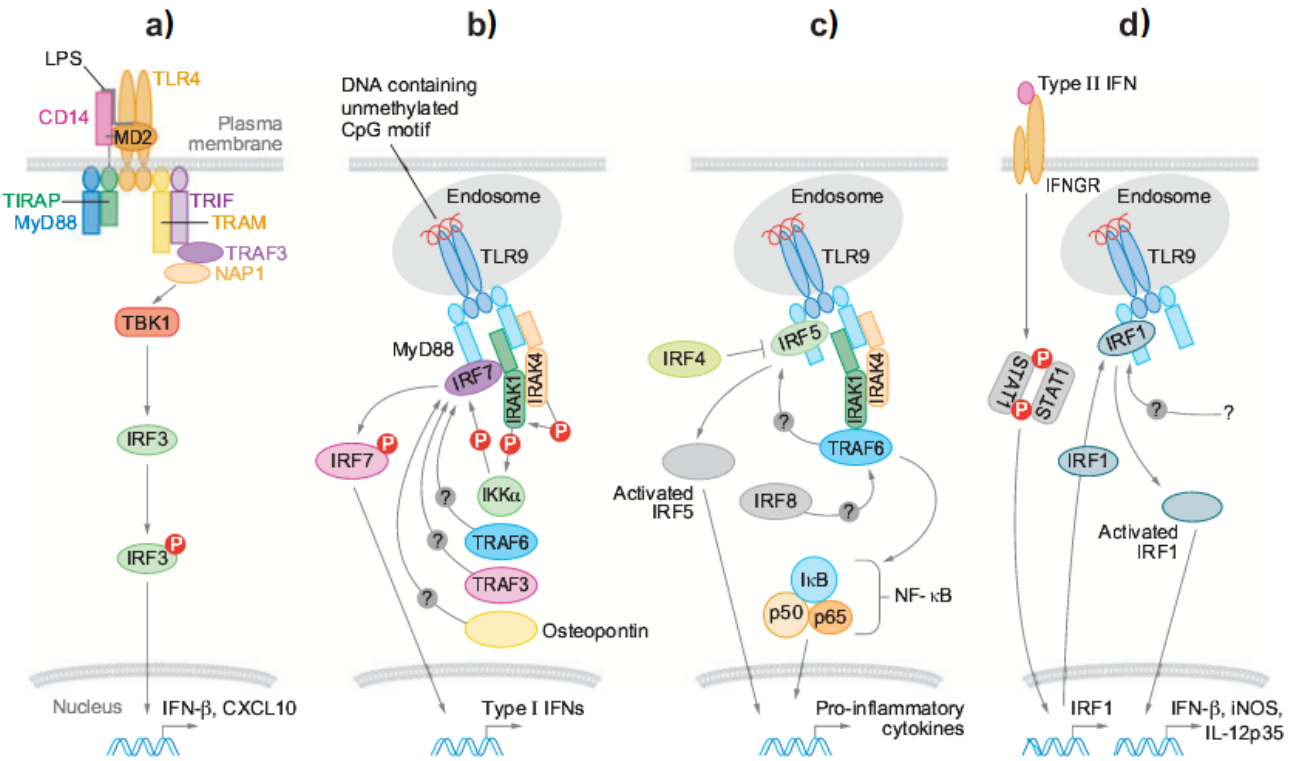

Figure 1.5: TLR-mediated IRF activation pathways in specific cell types. a) TLR4 signals through four adaptors, MyD88, TIRAP, TRIF, and TRAM with the associates with TBK1 through NAP1 and TRAF3. TBK1 mediates the phosphorylation (P) of IRF3 (and IRF7) for activating the expression of genes encoding IFN-β and CXCL10. b) IRF7 is directly phosphorylated and activated by binding to MyD88 in the endosomal compartment of stimulated TLR9 and action of IRAK1 and IKKα. IRF7 regulates the type I IFN gene. c) IRF5 and IRF8 are involved in this pathway and still unknown mechanism. Activated IRF5 translocates to the nucleus to activate proinflammatory cytokine gene. IRF4 also

involved in this pathway as inhibitor of IRF5 from binding to MyD88. d) IRF1 is induced via IFN-γ stimulation and dimerization of phosphorylated signal transducers and activators of transcription (STAT) 1. Induced IRF1 is activated and translocates to the nucleus to induce genes encoding IFN-β, inducible nitric oxide synthase (iNOS), and IL-12p35 by an unknown mechanism. Taken from (Tamura et al., 2008)

IRF-regulated cytokines are mainly induced through the activation of TLRs by viral, bacterial pathogens and their products (figure 1.5) (Tamura et al., 2008). The activated mechanism of IRFs is different from TLRs, cell types and ligands, and the mechanism for some pathways is still unknown. There are reports that stimulation of IFN genes (STING) and DNA-dependent activator of IRFs (DAI) can also induce type I IFN production in response to cytosolic DNA (Ishikawa, Ma, & Barber, 2009; Takaoka et al., 2007).

1.2.2 Reactive oxygen species

Oxidative stress is caused by various stimuli from the environment, including chemical oxidative and electrophillic agents such as drugs, xenobiotics, heavy metals and physical agents such as UV radiation. Oxidative stress will lead to the generation of reactive oxygen species (ROS) and electrophiles, which have a high impact on survival, growth development, and evolution of living organisms (Kaspar, Niture, & Jaiswal, 2009). Under infection, cells are also under stress conditions with various cytokines, chemokines, inflammasomes, and autophagy. This leads to the oxidative stress in cells (Tschopp & Schroder, 2010). ROS includes free radicals and oxidants, such as the superoxide anion (O_2^-), the hydroxyl radical (OH^-), and the hydrogen peroxide (H_2O_2). Cancer, renal/cardiovascular disorders, acute and chronic inflammation, respiratory diseases, and neurodegenerative diseases are the diseases that can be caused by ROS and electrophiles (H. K. Bryan, Olayanju, Goldring, & Park, 2013; Jaiswal, 2010; Kaspar et al., 2009).

To protect against these stress factors and to control the balance of the cellular redox state, eukaryotic cells have developed complex system to detoxify and maintain cellular homeostatics, which consists of four categories of several enzymes, such as thioredoxin, superoxide dismutases, glutathione peroxidases and catalases (Dinkova-Kostova, Holtzclaw, & Kensler, 2005; Jaiswal, 2010; Martinon, 2010). The nuclear factor (NF)-erythroid 2 (E2)-related factor 2 (Nrf2) is well established as the main mediator of cellular adaption to redox stress. Nrf2 is an ubiquitously expressed cap'n'collar (CNC) basic-region leucine zipper transcription factor that play an important role in drug metabolism, the oxidative stress response, cytoprotection, and many other bio-physiological processes (Hayes & McMahon, 2009; Motohashi & Yamamoto, 2004).

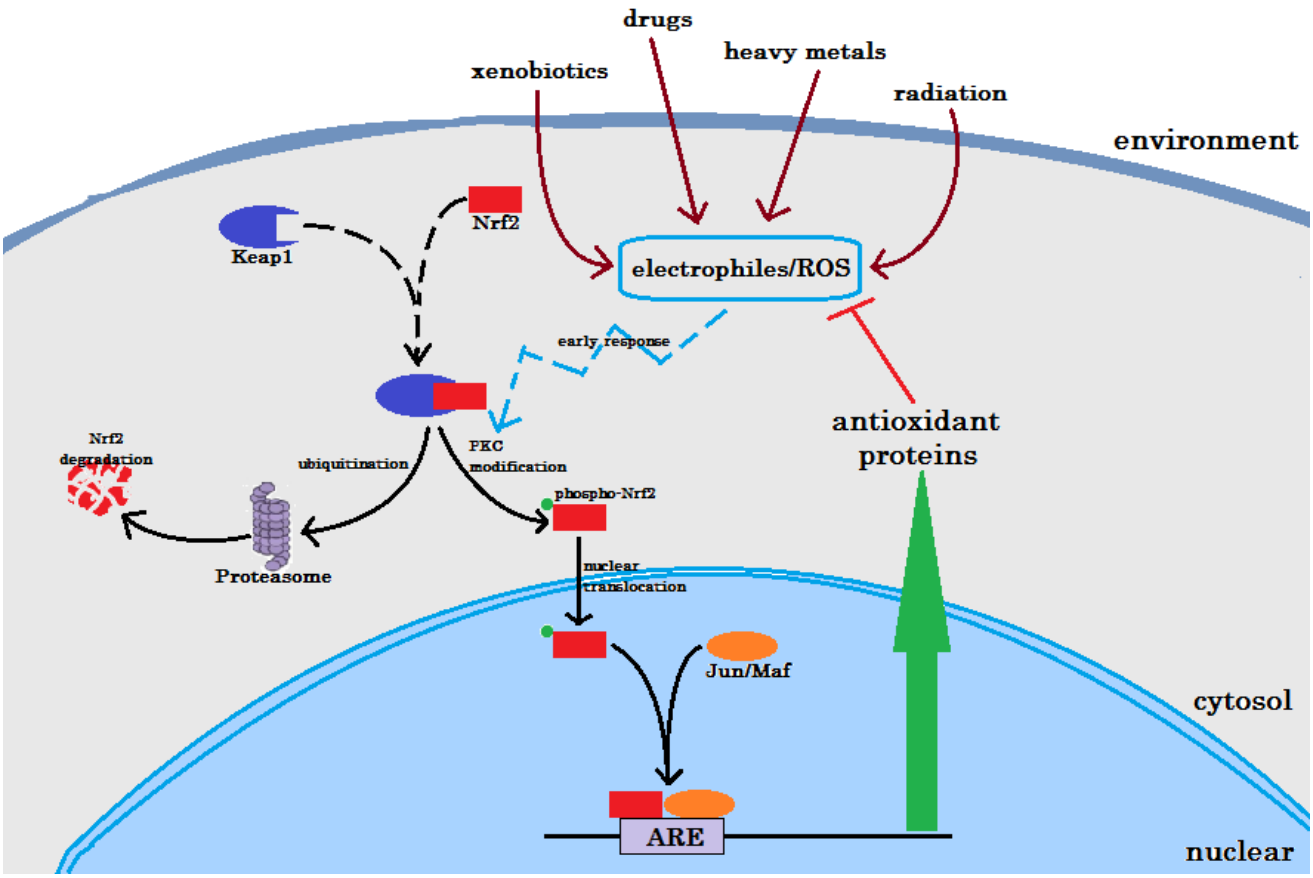

Figure 1.6: Overview of activation and inactivation of Nrf2 signaling pathway. In normal state, Nrf2 is directed to degradation by INrf2 (or Keap1) through ubiquitination. The ubiquitinated Nrf2 is guided to 26S proteasome for degradation. When stressed factors appear causing electrophiles or reactive oxygen species (ROS), Keap1 undergoes cysteine modification and Nrf2 is phosphorylated by protein kinase C δ (PKCδ). The result of this process is the dissociation of Nrf2-Keap1 complex. Free, active and stable phosphorylated Nrf2 translocates to nuclear. Together with small Jun/Maf molecule, the nuclear Nrf2 binds to antioxidant response element (ARE) for gene expression of antioxidant proteins, which will inhibit electrophiles or ROS.

In unstressed conditions, Nrf2 is maintained at low level in the cytosol by an inhibitor protein called inhibitor Nrf2 (INrf2) or Kelch-like ECH-associated protein 1 (Keap1), which acts as substrate adaptor to ubiquitinate Nrf2 and targets it for proteasomal degradation. Upon stress exposure, cysteine residues of Keap1 are activated leading to stop its Nrf2-inhibitor activity. Nrf2 is phosphorylated by protein kinase C δ (PKCδ), dissociated from Keap1 and translocated to the nucleus (figure 1.6). Stable nuclear Nrf2 binds to the antioxidant response element (ARE) with either small Maf or Jun for antioxidant gene expression, such as *NAD(P)H dehydrogenase*, *quinone 1* (*Nqo1*), *Glutathione S-transferase* (*Gst*) or *p62* for glutathione synthesis, elimination of ROS, detoxification of xenobiotics or drug transportation (reviewed by H. K. Bryan, Olayanju, Goldring, & Park, 2013).

1.2.3 Autophagy

Autophagy is the fundamental biological catabolic mechanism conserved in all eukaryotic cells and metazoan organisms. There are at least three types of autophagy: macroautophagy, microautophagy and chaperone-mediated autophagy. In general, autophagy is referred to macroautophagy. Autophagy is considered as a housekeeper, active at basal level in most cell types and strongly induced by starvation. It is very important for cells to maintain the integrity of intracellular organelles and proteins during normal state, and for cell survival during starvation that breaks down cellular components, like mitochondria, to maintain cellular energy levels. Autophagy involves self-degradation of unnecessary or dysfunctional cellular components to maintain the quantity and quality of intracellular biomass. It has been shown to contribute to cell survival and cell death through its interaction with apoptosis and necrosis (Deretic, 2012). Autophagy also has immunological role in the infection of microorganisms invading intracellularly (Deretic, 2009; Virgin & Levine, 2009). Several studies have shown that autophagy is one of the immunity and inflammation downstream outcomes of PRR signaling (Deretic & Levine, 2009), displaying a prominent property that can effectively eliminate intracellular bacteria, such as mycobacteria.

The hallmark morphological characteristic of autophagy which is different from phagocytosis is the formation of crescent-shaped slivers of membrane within the cytosol. The membrane wraps around cytoplasmic targets to generate a double membrane autophagosome that is converted into single delimiting membrane autophagolysosome upon fusion with late endosomal/lysosomal organelles. The autophagolysosome will degrade the captured material within it (Deretic, 2012). The autophagy begins with an isolation membrane derived from lipid bilayer, called phagophore. The phagophore forming may be contributed by the endoplasmic reticulum (ER) and/or the trans-Golgi and endosome, however it is still controversial (Axe et al., 2010; Simonsen & Tooze, 2009). This phagophore then is expanded and engulfs intracellular cargo, such as cytoplasmic protein aggregates, damaged organelles, or bacterial products, resulting in the formation of double-membrane autophagosome (Mizushima, 2007). The autophagosome is matured by fusing with lysosomes and the lysosomal acid proteases then degrade the autophagosomal content (Glick, Barth, & Macleod, 2010). This process will result in releasing amino acids and other by-products back to cytoplasm for re-used by cells.

However, autophagy is quite complex at the molecular level and a still ongoing focus for research. In general, after phagophore formation or nucleation, autophagy-related gene (Atg) 5 and

Atg12 conjugation together with interaction of Atg16L are multimerized on phagophores. This multimerization helps in the process of the microtubule-associated protein 1 light chain 3 (LC3), or known as Atg8, from LC3B i to LC3B ii then LC3B ii inserts into the phagophore membrane. This was described as a crescent-shaped membrane capturing proteins or organelles resulting in the autophagosome formation, which is fused with lysosomes to become autophagolysosomes containing lysosomal proteases (figure 1.7) (Glick et al., 2010). Autophagy is regulated by both external and internal factors. The internal one includes stress-signaling kinases such as c-Jun N-terminal kinase (JNK) 1 or mitogen-activated protein kinase 8 (MAPK8), which will phosphorylate B-cell lymphoma (Bcl-2) and thus inhibit the interaction of Beclin-1 with VPS34, a class III phosphoinositide (PI) 3-kinase (PI3K), resulting in the promotion of autophagy. Another internal factor is mammalian target rapamycin (mTOR), an endogenous inhibitor of autophagy, which is inhibited by external factors, such as low energy, hypoxia or stressed factors; or promoted by the insulin receptor and its adaptor through reducing or increasing guanosine triphosphate (GTP)-binding protein Rheb activity, respectively (reviewed by Glick et al., 2010).

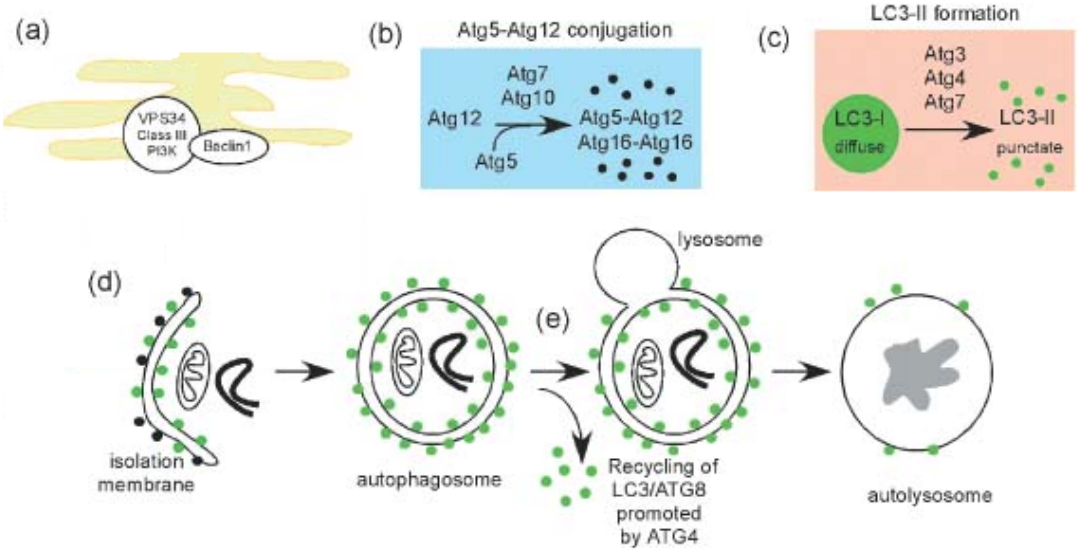

Figure 1.7: Molecular signaling in autophagy. (a) phagophore formation or nucleation contributed by endoplasmic reticulum (ER) and/or the trans-Golgi and endosomes via signal from Beclin1-VPS34 interaction, (b) multimerization of Atg5 and Atg12 conjugation together with interaction of Atg16L at phagophores, (c) the LC3 processing from LC3B i to LC3B ii inserts into the phagophore membrane, (d) capture of proteins or organelles for degradation, the completion of autophagosome will release some LC3ii/Atg8 promoted by Atg4 for recycling, and autophagosome fuses with lysosome to become autophagolysosome for lysosomal proteases. Taken and modified from (Glick et al., 2010)

1.3 *Keap1* – the interplay factor in the innate immune system

1.3.1 Structure of Keap1

As mentioned previously, Nrf2 is the critical factor that regulates the cellular defense against oxidative stresses; and Keap1, or INrf2, is the negatively cytosolic regulator of Nrf2, to maintain the balance during basal state and prevent the over-activation of Nrf2. The identification of an inhibitor of Nrf2 was first announced by Itoh and colleagues in 1999 (Itoh et al., 1999). Later, many studies about this molecule arose and gave more characteristics for this Keap1 molecule (reviewed by H. K. Bryan, Olayanju, Goldring, & Park, 2013). Keap1 exists as a homodimer binding one Nrf2 and it has three major domains (figure 1.8). The N-terminal BTB (broad complex, tramtrack, bric-a-brac)/POZ (poxvirus, zinc finger) is the protein-protein interaction domain containing the Cys151 residue, which binds to Cullin 3 (Cul3)/RING-box protein 1 (Rbx1) E3 ubiquitin ligase complex. This domain also acts as the stress-sensing domain. The linker region, or intervening region (IVR), is cysteine-rich domain consisting Cys273 and Cys288. This region contributes to the activity of Keap1 as the second stress-sensing domain (Ogura et al., 2010). The C-terminal Kelch domain (CTR) is linked with a double glycine repeat (DGR) containing six conserved Kelch repeat sequences forming a β-propeller structure. This domain is where the Keap1 binds to Nrf2 through the Neh2 domain on Nrf2. In normal state, the Keap1 serves as an adapter for Cul3/Rbx1 E3 ubiquitin ligase complex and leads to the ubiquitination and degradation of Nrf2 through the 26S proteasome.

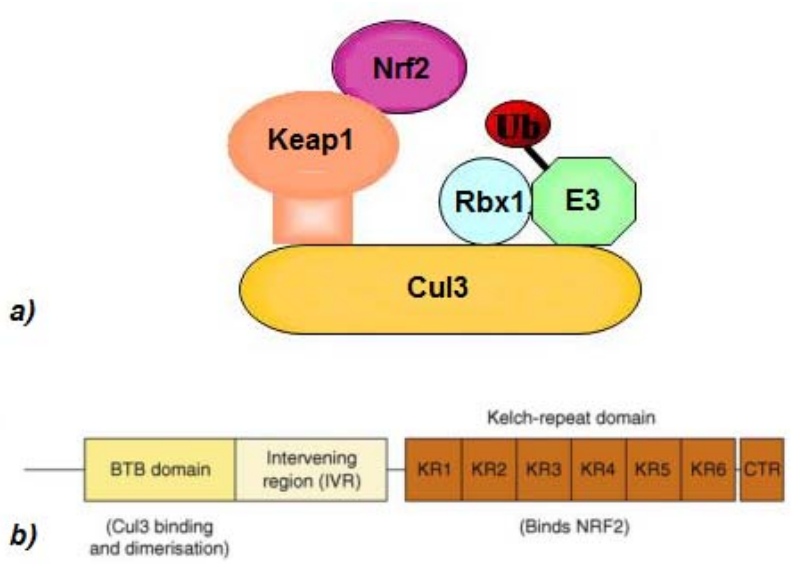

Figure 1.8: Structure of Keap1 (or INrf2). a) Represented 3D-structure of Keap1 structure binding Nrf2, taken and modified from (Zhang et al., 2005). b) The arrangment of protein with three major domains. The N-terminal BTB (broad complex, tramtrack, bric-a-brac) domain is responsible for Cul3/Rbx1 E2 ubiquitin ligase complex binding. The intervening region (IVR) distributes to the activity of Keap1. These two BTB and IVR consist important cysteine residues for stress sensing. And the C-terminal with 6-repeated-Kelch domain/double glycine repeat (DGR) has function of binding to Neh2 region on Nrf2, taken from (Hayes & McMahon, 2009)

From the time it was discovered, there are many studies showing the role of Keap1 as a key element in cancer treatments. In the hypothesis paper, Stepkowski showed an interest in the molecular cross-talk between the Nrf2-Keap1 signaling pathway with autophagy and apoptosis (Stepkowski & Kruszewski, 2011). Most recently, Tian and others also give a mini review on the multi-functional Keap1 on "killing three birds" which are Nrf2, IKKβ and Bcl-2 in ROS, inflammatory and autophagy, respectively (figure 1.9) (Tian et al., 2012).

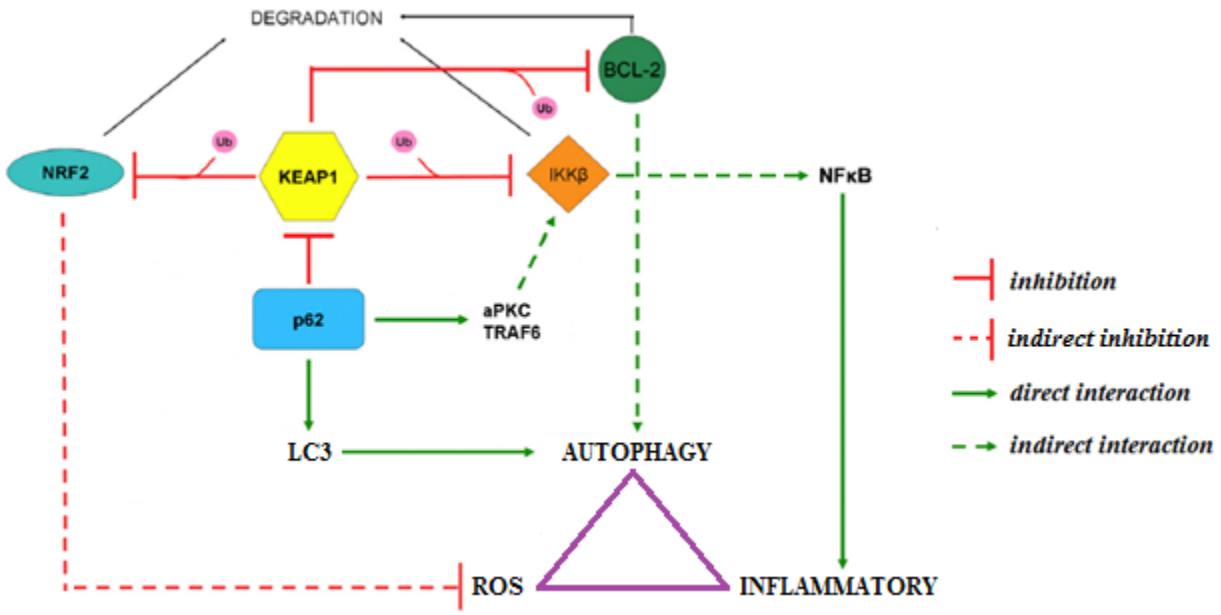

Figure 1.9: Mechanism of Keap1 as interplay factor of oxidative stress, autophagy and inflammatory. Keap1 has direct interaction with IKKβ, Bcl2 and Nrf2 and guides them for ubiquitination (Ub). p62 has negative effect on Keap1 through binding. So that, Keap1 indirectly participates in the ROS, inflammation and autophagy. Taken and modified from (Stepkowski & Kruszewski, 2011)

1.3.2 Keap1 and Nrf2 in ROS

Several studies have shown the importance of Keap1 in Nrf2 regulation. Wakabayashi and others proved the significant role when they ablated *Keap1* in mouse (Wakabayashi et al., 2003). They showed evidence that Nrf2 constitutively accumulated in the nucleus and stimulated transcription of cytoprotective genes and produced phase II detoxifying enzymes. And mice with Keap1-deficiency died postnatally. More examinations showed the hyperkeratosis in esophagus and forestomach, together with the induction of keratin K1, K6 and loricrin. Sykiotis and Bohmann added more to Keap1's importance with studies on Drosophila (Sykiotis & Bohmann, 2008). It is shown that Drosophila males with *Keap1* loss-of-function mutation had longer life-time and higher tolerance to oxidative stress than others. Many studies about cancers also state the importance of Keap1 in

Nrf2-interaction. It was reviewed by Hayes that Nrf2 is accumulated and mutated due to dysfunction Keap1 in lung, breast, and bladder cancers causing problems in prognosis (Hayes & McMahon, 2009; Kaspar et al., 2009). The most recent study from Williamson and Johnson showed the increase of Nrf2 both *in vitro* and *in vivo* experiments when *Keap1* was knockdown by siRNA (Williamson, Johnson, & Johnson, 2012). The up-regulated activation of Nrf2-ARE pathway increased the protection against oxidative stress in primary astrocytes, and also protected against 1-methyl-4-phenyl-1,2,3,6-tetrahydropyridine (MPTP)-induced dopaminergic neuron damage/loss in mice.

1.3.3 Keap1 and IKKβ in inflammatory pathway

Recently, IKKβ was identified as another substrate for the Keap1-Cul3-E3 ligase complex that influenced the expression of NF-κB (Kim et al., 2010; Lee et al., 2009). They showed that IKKβ contains an E(T/S)GE motif similar to the one of Nrf2 and Keap1 binds to IKKβ through the same DGR region directly (Kim et al., 2010; Tian et al., 2012). In one study, Kim and others stated that only IKKβ in the IKK complex had an interaction with Keap1, although IKKα and IKKβ have similar structures with 70% amino acid homology and may form heterodimers together (Kim et al., 2010). With the Keap1-binding, IKKβ was a substrate for Cul3-E3 ligase and guided to degradation by autophagy. At the same time, the IKK phosphorylation stimulated by TNFα also was inhibited. Moreover, IKKβ is one of the IKK complex molecule, and an important molecule in NF-κB signaling pathway. The transcription factor NF-κB is activated through the releasing of IκB induced by phosphorylated IKK complex. It had been proven in these studies that Keap1-IKKβ had effect on NF-κB expression. Lee *et. al*. made Keap1 depletion and observed up-regulation of NF-κB-derived tumor angiogenic factors (Lee et al., 2009). Meanwhile, Kim *et. al.* made an introduction of Keap1 gene and NF-κB reporter gene into HEK293 cells, they observed that NF-κB activity was inhibited. And knockdown *Keap1* gene gave a higher basal signal of TNFα-induced activity compared to control cells (Kim, 2010). Overall, Keap1 and IKKβ interaction has an effect on NF-κB which is one of the inflammatory signaling pathways. Thus, the Keap1 actually contributes to the signaling in inflammation.

1.3.4 Keap1 and Bcl-2 and p62 in autophagy

Bcl-2 is B-cell lymphoma 2, which was first discovered as a regulatory protein regulating cell death or apoptosis. Later, it was shown that Bcl-2 also is a multifuctional protein influencing many cellular processes (Pattingre & Levine, 2006). Bcl-2 has been known with antiapoptotic and antiviral

effects on preventing virus-induced cell death and restricting viral replication (Liang et al., 1998). In 1998, Liang showed the interaction of Bcl-2 with Beclin in controlling the cell death. It was proven that the interaction between Beclin and Bcl-2 family protein, especially Bcl-x_L, induced death repressor activity. In 2005, Pattingre and colleagues added the antiautophagic effect to Bcl-2 functional profile through interaction with Beclin-1 (figure 1.10) (Levine, Sinha, & Kroemer, 2008; Pattingre et al., 2005). In addition to information of Beclin-1 responsible for autophagosome formation in autophagy, the experiments between wild-type Beclin-1 and unbound-Bcl-2-mutated Beclin-1 gave key finding that Bcl-2 inhibits both Beclin-1-dependent autophagy and autophagic cell death (Pattingre & Levine, 2006; Pattingre et al., 2005).

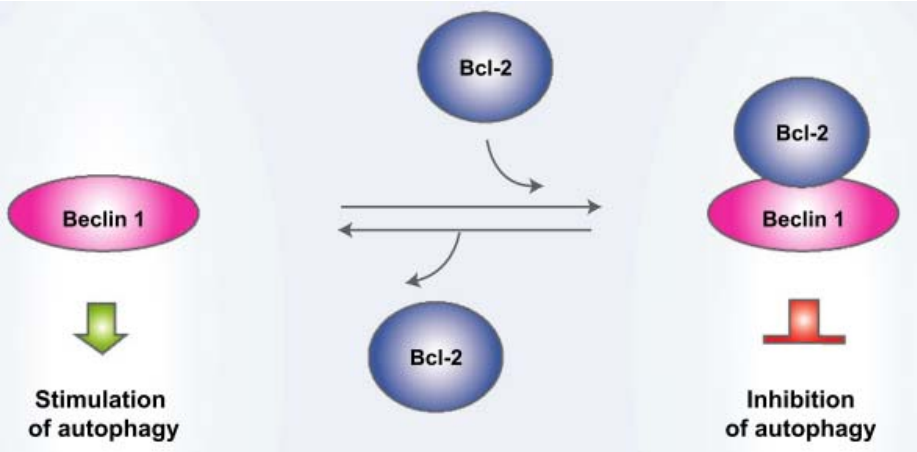

Figure 1.10: Interaction between Beclin-1 and Bcl-2 affects autophagy. Beclin-1 is responsible for autophagosome formation in autophagy pathway. Bcl-2 interaction with Beclin-1 inhibits it function and autophagy is inhibited. Taken and modified from (Pattingre & Levine, 2006)

Recently, Niture and Jaiswal had shown the interaction between Bcl-2 and Keap1 through cell line models (Niture & Jaiswal, 2010). Structure of Keap1 protein has multi-binding domain DGR, which binds to Bcl-2 at BH2 domain. The interaction of Bcl-2 to Keap1 has the same outcome as Nrf2 and IKKβ which leads to the degradation of Bcl-2. The Bcl-2 was ubiquitinated by Keap1-Cul3-Rbx1 complex at N-terminal lysine 17 in both *in vitro* and *in vivo*. In normal state with the overexpression of Keap1, the Bcl-2 is targeted for degradation which increases Bax molecules and decreases Bcl-2-Bax complex in cells (figure 1.11). While Bcl-2-Bax complex is the suppressor for cytochrome c (CytC), the main factor that activates caspase enzymes for DNA fragmentation and cell apoptosis, released from mitochondria, the Bax molecules help to open the mitochondrial voltage-dependent anion channel (VDAC) for CytC releasing (Shi et al., 2003). Then, the overexpression of Keap1 caused increase in cell apoptosis. It has been shown previously that Bcl-2 has its function in

autophagy with interacting with Beclin-1, hence the Keap1 might have indirect interaction with autophagy through Bcl-2.

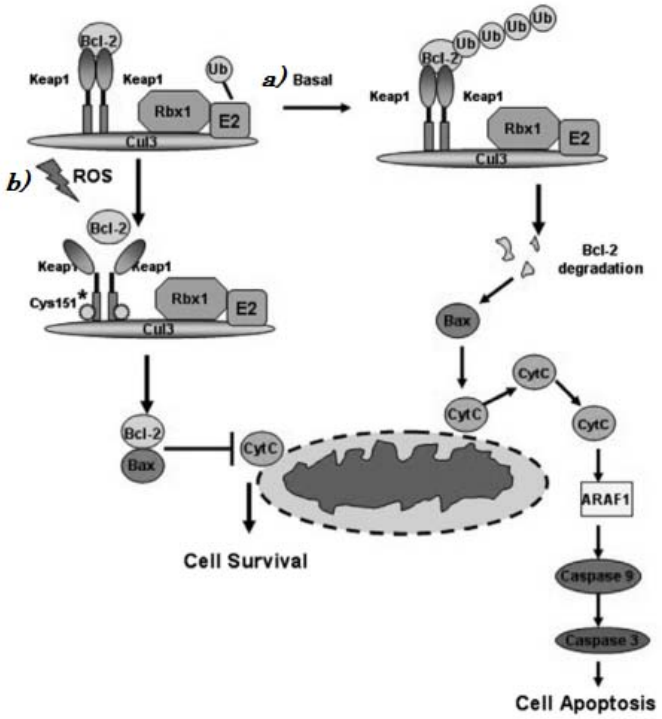

Figure 1.11: Schematic model of Keap1 regulating Bcl-2 family. a) Under the basal condition, Keap1 interacts with Bcl-2 and targets to degradation of ubiquitinated Bcl-2 by Keap1-Cul3-Rbx1 E3 ligase complex, following the accumulation of Bax and subsequent release of cytochrome c (CytC) from mitochondria, activation of caspase 9, 3 leading to cells apoptosis. b) When ROS appears, Bcl-2 is dissociated from Keap1-Cul3-Rbx1 E3 ligase complex making heterodimers with Bax, which are suppressors to the release of CytC, resulting in cell survival. Taken from (Tian et al., 2012)

Many studies have reported the role of p62, also called Sequestosome 1 (SQSTM1), as a linking polyubitinated protein to the autophagic system (Bjorkoy et al., 2005; Pankiv et al., 2007). p62 is involved in various cellular processes by serving as a molecular hub mediating various protein-interaction (Jin et al., 2009; Moscat & Diaz-Meco, 2006). Multidomain adaptor p62 protein binds to various signaling proteins, including Keap1-interacting region and TRAF6 binding site (figure 1.12), for oligomerization and forming cytosolic speckles (Stepkowski & Kruszewski, 2011). Structural p62 consists of Phox and Bem1p (PB1) domain in N-terminal region, which is the protein-protein interaction domain. The PB1 domain mediates the binding of other proteins such as neighbor of BRCA1 gene 1 protein (NBR1), mitogen-activated protein kinase (MEK) 5, extracellular signal-regulated kinase (ERK), a protein kinase C (PKC) as well as oligomerization. Along the p62 protein, there are two regions responsible for apoptosis signaling including a zinc finger (ZZ) domain for

ribosome inactivating protein 1 (RIP1)-binding site and a TRAF6-binding site (review by Stepkowski & Kruszewski, 2011). p62 is participating in autophagy through the LC3-interacting region (LIR) (Pankiv et al., 2007). An antioxidant signaling of p62 is showed through Keap1-interacting region (KIR), similar to Nrf2, thus p62 acts as a Keap1 binding competitor with Nrf2 (Komatsu et al., 2010). And at the C-terminal region is the ubiquitin (Ub) associated (UBA) domain binding non-covalently to poly-ubiquitinated protein for proteasomal degradation (Seibenhener et al., 2004; Wooten et al., 2006). p62 with this structure guides the bound proteins to autophagy and lysosome for degradation. p62 also acts as a bridge between Keap1 and LC3B ii in autophagy, thus, Keap1 again might have interaction with autophagy via p62 (Komatsu et al., 2010; Lau et al., 2010).

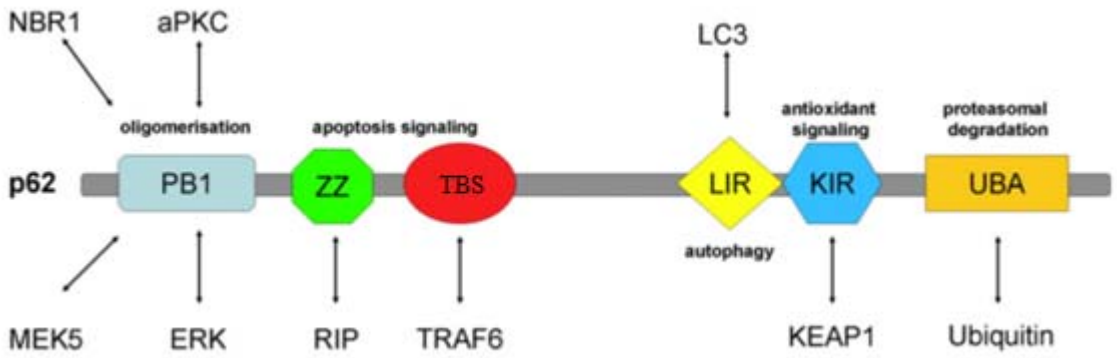

Figure 1.12: Structure of multidomain p62 protein. PB1: Phox and Bem1p, protein-protein interaction domain binding with proteins. ZZ: zinc finger RIP1-binding domain, TBS: TRAF6 binding site, LIR: LC3-interacting region, KIR: Keap1-interacting region, UBA: polyubiquitin-biding domain. Taken and modified from (Stepkowski & Kruszewski, 2011)

Overall, Keap1 might have a role as a link between ROS, inflammation and autophagy. And these pathways have an important role in controlling *M. avium* infection. The question here is whether and how Keap1 has an effect in controlling *M. avium* infection through the interplaying of different innate immune pathways.

2. Aim and objectives

The overall aim of this study was to investigate the immune response mechanism and killing of *M. avium* in human primary macrophages. Given the proposed roles of Keap1 in oxidative stress, autophagy and inflammation, the main goal was to investigate the role of Keap1 in the regulation of inflammation and autophagy as well as mycobacterial survival, especially in *M. avium* infection. Specifically, Keap1 was knocked down in primary human monocyte-derived macrophages (MDMs) to observe its actual role between signaling pathways during *M. avium* infection by:

1. Examining the role of Keap1 in inflammatory signaling by measuring phosphorylated and total proteins of select inflammatory signaling pathways in *M. avium*-infected macrophages with and without Keap1 knockdown.
2. Examining the role of Keap1 in the regulation of autophagy in *M. avium*-infected MDMs.
3. Investigating the effect of Keap1 on the intracellular survival of *M. avium* in infected MDMs.
4. Optimizing a quantitative PCR method for detection of mycobacteria in infected macrophages.

3. Methodology

3.1 Cells

The human monocyte-derived macrophages (MDMs) were isolated by density centrifugation from fresh buffy coats provided by The Blood Bank of St. Olavs Hospital, Trondheim, Norway. The use of peripheral blood mononuclear cells (PBMCs) from healthy blood donors is approved by the Regional Committees from Medical and Health Research Ethics at NTNU after informed consent. Due to their natural features that can represent accurately the responses of human immune system, the primary MDMs were chosen for this project.

The buffy coat was mixed with 100ml of sterile preheated Phosphate Buffered Saline (PBS) (Sigma Aldrich, USA) at 37°C and transferred to the 50ml-conical tubes containing 15ml of density gradient solution Lymphoprep^{TM} (Axis-Shield). The tubes were spinned down with 1800rpm for 20 minutes at 20°c with no brake. The PBMCs, remaining in the white layer between Lymphoprep^{TM} and plasma, were carefully taken to new tubes for spinning down again with 2000rpm in 10 minutes to get the pellets. The PBMCs were washed 4 times with warmed Hanks Balanced Saline Solution (HBSS) (Sigma Aldrich, USA) by centrifuging in 8 minutes with 800rpm. The final PBMCs solution was counted for diluting suitable concentration. 20µl of cell solution was diluted in 10ml of isoton and 1 drop of zapoglobin to prevent cell clump. The profile B (with T1 = 30,000fl and Tu = 32,000fl) of Coulter particle count and size analyzer Z2 (Beckman Coulter) was used to count the number of cells based on size, including monocytes, lymphocytes and natural killer-cells. The cells were diluted in cell culture medium Roswell Park Memorial Institute (RPMI) 1640 (Sigma Aldrich, USA) containing 5% corresponding serum provided by the Blood Bank (St. Olavs Hospital) to get 5x10^{6} cells/ml. The 500ml- RPMI 1640 contains 1.7ml of L-glutamine and has 5mM Hepes solution (Life Technologies). The diluted total PBMC solution is seeded to suitable plastic cell-culture plates and let the cells attach for 1 hour in incubator with 37°C and 5% CO_2 to allow the adherence of monocytes. After that, the plates were washed 3 times with warmed HBSS and changed medium to 30% serum RPMI for macrophages differentiation. The macrophages will be derived from monocytes within 3-5 days when they are incubated at 37°c and 5% CO_2. The stimulation and infection were taken in 10% serum RPMI after differentiation.

3.2 Mycobacterial culture

Mycobacterium avium strain 104 stably expressing firefly luciferase (kind gift from David R. Sherman), which is described elsewhere (Halaas et al., 2010), was used for all the experiments in this thesis project. The morphology of this strain is smooth and transparent (SmT) type. This *M. avium* strain 104 has fulfilled some criteria of pathogenic mycobacteria. It was originally isolated from an AIDS patient with relatively stable genome and easy for transformation (Saunders, Dane, Briscoe, & Britton, 2002).

One mycobacterial colony was picked from stock plates and grown in 5-10ml of Middlebrook 7H9 broth medium (Difco/Becton Dickinson) containing glycerol, Tween 80, and albumin dextrose catalase growth supplement (ADC) on shaker at 37°c for 3-5 days. We estimated the number of mycobacteria by measuring OD at 600nm and used the bacteria for infection at between 0.3 to 0.6 (when the growth is at log phase) when the mycobacteria is in the most active stage. The approximate number of bacterial cells per milliliter is calculated by multiplying the OD600 result with 4.5×10^{8}. The mycobacterial counts were quantified by plating with appropriate dilution on Middlebrook 7H10/OADC agar (Difco/BD) for counting colony-forming unit (CFU) and by luciferase report assay for luminescence activity (the Luciferase Reporter 1000 Assay System, Cat. #E4550, Promega).

3.3 *Keap1* siRNA transfection assay

Small interfering RNA (siRNA), or short interfering RNA, or silencing RNA is a class of double-stranded RNA (dsRNA) molecules, which has 20-25 base pairs in length. It is first discovered in post-transcriptional gene silencing (PTGS) in plants, and now is used in the gene silencing technique based on the role of interfering with the expression of specific genes with complementary nucleotide sequences. siRNA is often introduced in cell lines through transfection or electroporation. When it is in the host cell, it will become a part of the RNA-induced silencing complex (RISC) and degrade target mRNA. This process is guided by the antisense strand of the siRNA followed by the result of inhibiting mRNA translation, that is illustrated by figure 3.1.b). The success of RNA interference (RNAi) is depended on the appropriate delivery concentration of siRNA and time of treatment when it may bring the maximum expected response. In some cases, the siRNA delivery fails when the vertebrate cells detect the presence of a long dsRNA as antiviral component and then the cells will go through apoptosis.

In this project, we used lipid transfection as the method to deliver siRNA to human MDMs. It is advantageous in delivering DNA of all sizes, RNA and protein into wide range of cell types with high efficiency and a relatively low cost. This comprises cationic liposomal reagents consisting of a positively charged head group, a flexible linker group and two or more hydrophobic tail groups. The principle of the delivery of siRNA using this cationic lipid reagent is described in figure 3.1.a). The screening experiments for effective knockdown were performed by our laboratory researchers previously. Human MDMs were cultured on 6-well tissue-cultured plates (NUNC) with 30% serum RPMI free of antibiotics. Transfection with siRNA was performed after 1 week of seeding cells for macrophage differentiation followed the RNAi transfection protocol of Invitrogen™ for Lipofectamine® RNAiMAX reagent (# 13778-150). While the Opti-MEM®1 (1X) (#11058-021) is from Gibco®, the AllStar Negative control (#1027281) and *Keap1* Gene solution siRNAs (#1027416) are from QIAGEN with detailed information in table 3.1.

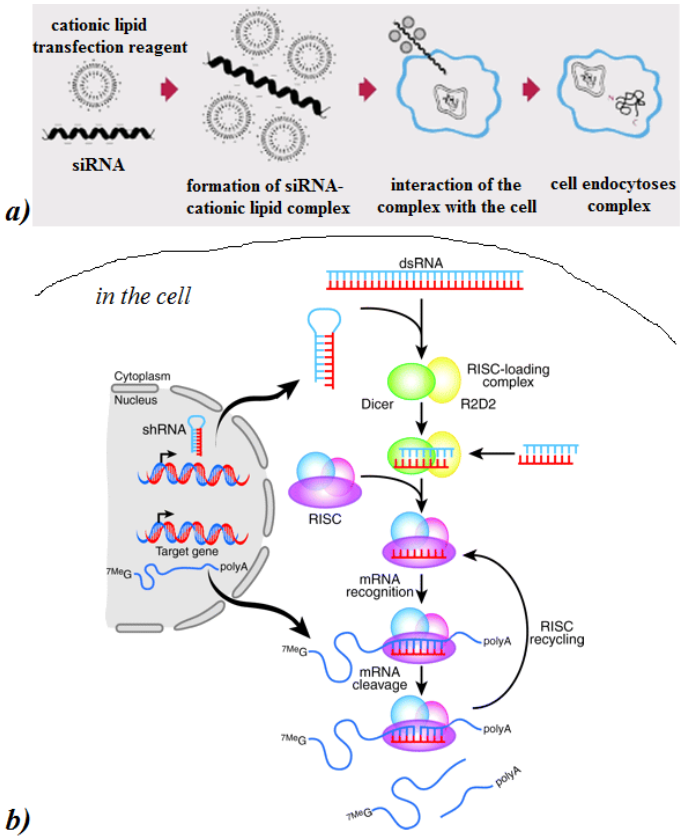

Figure 3.1: Principle of siRNA transfection. a) is the principle of lipid transfection (taken and modified from Life technologies™). When the complex of siRNA and cationic lipid transfection reagent is made, the complex will interact with cell and be endocytosed by cell. When getting inside, the siRNA will be released from the complex and take action in inhibiting mRNA, which is illustrated by b), RNAi-mediated gene silencing, taken from (Dominska & Dykxhoorn, 2010). The siRNA here can be dsRNA or shRNA, which can be derived from long precusor RNA molecules by the cell or introduced into the cells, will be taken up by the multisubunit RNA-induced silencing complex (RISC). The Ago2 protein, the central component of RISC, will unwind siRNA and bind antisense strands. The antisense RNA strand will guide RISC to complementary site in the target mRNA, resulting in mRNA cleavage. The antisense siRNA strand-loaded RISC is recycled for several rounds of mRNA cleavage. shRNA: small hairpin RNA, R2D2: enzyme of RNA silencing, 7MeG_polyA: mRNA.

Table 3.1. *Keap1* siRNA sequences.

Name	No.	Sequence	Features
Hs_KEAP1_2	SI00451675	CCGGGAGTACATCTACATGCA	coding DNA sequence
Hs_KEAP1_5	SI03246439	CCAGGATGCCTCAGTGTTAAA	exon
Hs_KEAP1_6	SI04155424	CAGCTGTCACCATGTGATTTA	exon
Hs_KEAP1_7	SI04267886	CTCCAGCGCCCTGGACTGTTA	exon

Only 7-day macrophages with healthy cells and 75% of confluence were procceed for transfection. It was twice at 0 and 48 hours and treated for 72 hours with 20nM siRNA. The reaction mixtures were made according to the manufacturer's protocol. The negative control was cells transfected with non-target AllStar siRNA, and the Hs_KEAP1_pool of four siRNAs was used to target *Keap1* mRNA. The *Keap1* knockdown was evaluated by western blotting. The viability of transfected cells was also evaluated.

3.4 *In vitro* infection and time-course experiments

The mycobacteria from broth cultures which have OD600 between 0.3 and 0.6 were collected by centrifuging at 10000rpm for 2 minutes. The collected pellet was washed with PBS with centrifugation at 10000rpm for 2 minutes. Then, the washed pellet was dissolved and sonificated in PBS thrice for 30 seconds each time to remove clumping of bacterial cells before infection. A multiple of infection (MOI), which represents the number of mycobacteria cells over one human cell, was calculated for appropriated response and added to the macrophages with and without gene knockdown.

The cells with gene knockdown and siRNA negative control treatment were removed siRNA media and incubated with 10% serum RPMI at 37°c, 5% CO_2 in 1 hour before *M. avium* infection. The infection was taken in within 4 hours for assessing inflammatory responses; while the excess mycobacteria were washed away after 4 hours of infection and continued incubating in 10% serum RPMI in 24 hours and 72 hours for autophagy and intracellular survival experiments. For LC3 assessment of autophagy, Bafilomycin A1 (BAF-A1) (Sigma aldrich, USA) was added with a concentration of 100nM before the sample collection for 2 hours. In normal basal condition, the formed LC3B ii proteins in autophagosome will then be partly degraded when lysosome fusion occurs, causing a difficult and incorrect assessment of autophagy formation. BAF-A1 is a specific

inhibitor of vacuolar type H^+-ATPase in the cells and it can inhibit the acidification of organelles, leading to the blocking of autophagosome-lysosome fusion (figure 3.2). The LC3ii proteins formed by autophagy processes are then not degraded as normal basal condition.

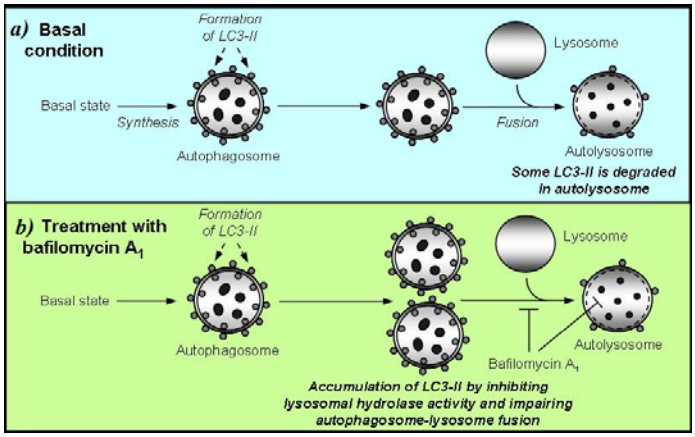

Figure 3.2: Mechanism of action of bafilomycin A1 (BAF-A1) in autophagy. a) shows the normal rate of autophagsomes and autophagosome-lysosome synthesis under basal condition. The LC3ii formation at the early stage of autophagosome will be partly degraded when lysosome fuses with autophagosome forming autophagolysosome. b) shows treatment with BAF-A1, which inhibits lysosomal hydrolases and then subsequently blocks autophagosome-lysosome fusion. This will result in preventing LC3ii degradation and an increase in LC3ii level comparing to the basal state. (taken from Sarkar)

3.5 Western blotting

Standard procedures of western blotting were performed for assessing proteins levels in MDMs. The sample experiments with *Keap1* gene knockdown were used with negative control of cell-without *Keap1* gene knockdown.

3.5.1 Basic principles

There are several methods for detecting total proteins in general and phospho-proteins in specific, such as Kinase activity assay, Phospho-specific antibody development, Western blotting, Enzyme-linked immunosorbent assay (ELISA), Cell-based ELISA, Intracellular flow cytometry and immunocytochemistry/immunocytohistochemistry, Mass spectrometry, or Multi-analyte profiling… Here, in this project, we chose western blotting for identifying interesting proteins.

Immunoblotting, or western blotting, is used widely and popularly in biomedical science as cheap and simple technique. The basic principle is illustrated by figure 3.3. By running cell lysate on sodium dodecyl sulfate polyacrylamide gel electrophoresis (SDS-PAGE), the proteins are separated from one another according to their size, or molecular weight. After running, the proteins are tranferred to either nitrocellulose or polyvinylidene flouride (PVDF) membrane by either wet or semi-dry transfer based on their electrical charge property. The interesting proteins will be detected

by incubation with specific antibodies against proteins and visualized by either chemiluminescence or fluorescence.

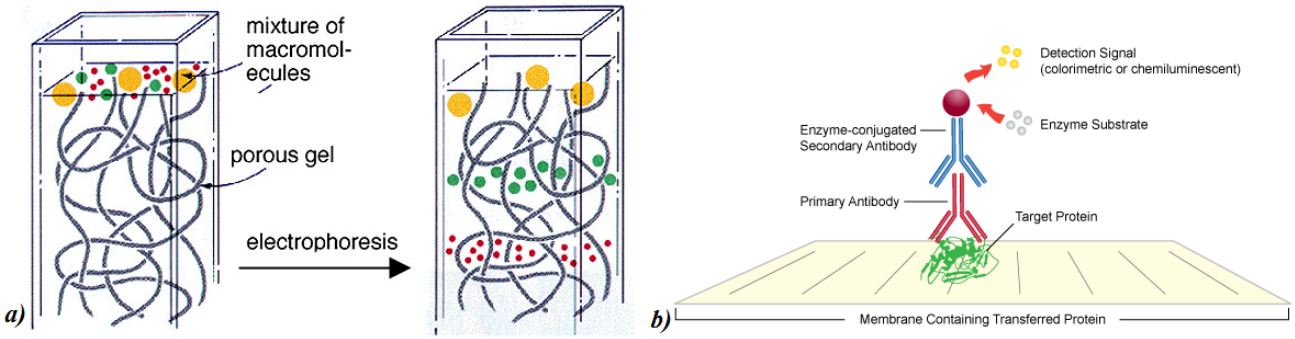

Figure 3.3: Basic principles of the western blotting. In a), the sodium dodecyl sulfate polyacrylamide gel electrophoresis (SDS-PAGE) is used to separate the protein mixture into different bands based on their travelling through the gel, which is depend on their molecular mass. The proteins at the upper band will have large molecular weight, which are inconvenient to travel through the matrix of gel and travel slower than the small proteins, which are at the lower bands. b) illustrates how the interesting proteins are defined and quantify, by primary antibody against interesting protein, enzyme-conjugated secondary antibody against primary antibody, and substrate reacting with conjugated enzyme on secondary antibody. (Leinco)

3.5.2 Standard procedures

The basic procedure is illustrated by figure 3.4.

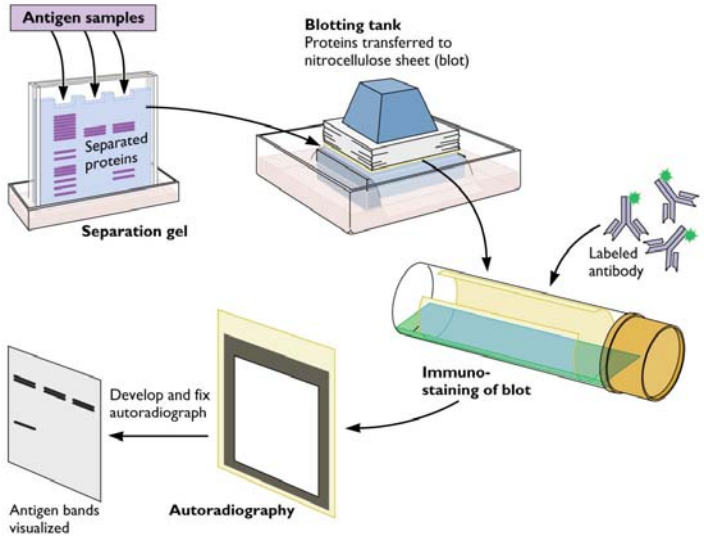

Figure 3.4: Basic procedure of western blotting. The antigen samples here are the interesting proteins samples which will be detected by antibodies against proteins. The gel separates proteins according to their size, then they are transferred to membrane, which are called blotting step. The labeled antibodies are used to bind with interesting protein, so that they can be detected by autoradiography after developing.

Cellular lysate collection: The cells were washed with ice-cold PBS twice and lysed in cold lysis buffer (appendix 2: Buffers and solutions used in the study) containing cOmplete, Mini, EDTA-free Protease Inhibitor cocktail (#11836170001) from Roche Applied Science (Switzerland) and 0.25U/ml benzonase nuclease (Novagen, USA) for bulky DNA cutting. The cell lysis samples were

kept on ice during 10 minutes of lysis buffer incubation. 3 periods of sonification were done with votexing in between for complete lysation. The cell lysis was centrifuged at 10000rpm for 20 minutes at 4°c. The supernatant was collected for western blotting or storing at -80°c in long term.

SDS-PAGE running: A 16µl of total protein lysate was mixed with 6µl of NuPAGE® LDS Sample buffer 4X containing 0.1M dithiothreitol (DDT) (Invitrogen™, USA) and heated at 70°c in 10 minutes for reduced and denatured proteins. 20µl of mixed protein was loaded in each well of NuPAGE® Novex® 10% Bis-Tris Gel with 1X NuPAGE® MES SDS Running buffer containing antioxidant (Invitrogen™). To determine the running of the protein size, 5µl of SeeBlue® Plus2 Pre-Stained Standard (Invitrogen™) was loaded into the marker well for molecular weight marker. The gel was run with 2 conditions: 30 minutes at 100V and then 90 minutes at 150V, which were optimized by Awuh previously.

Transferring the proteins from gel to nitrocellulose membrane: This procedure was done following the protocol of Invitrogen™'s iBlot dry blotting system with 20V in 9 minutes. After transferring the proteins, the membrane was washed with Tris Buffered Saline-with Tween-20 (TBS-T) under agitation in 5 minute 1 time.

Blocking the membrane: The nitrocellular blot was blocked in 1 hour under agitation with 5% non-fat milk in TBS-T or 5% bovine serum albumin-fraction V (BSA) in TBS-T. Then the blot was washed 3 times in 5 minutes under agitation with TBS-T to remove excess milk or BSA of blocking before incubating with primary antibody.

Primary antibody incubation: The primary antibody against interesting proteins was diluted in 5% non-fat milk or 5% BSA in TBS-T with ratio 1:1000. The incubation was taken overnight(s) or more than 18 hours under 4°c and gentle agitation. With one exception, the incubation with anti-GAPDH primary antibody was taken within 30 – 60 minutes at room temperature under agitation.

Secondary antibody incubation: The incubated blot was washed 3 times with TBS-T in 5 minutes under agitation with TBS-T to remove excess and unbound primary antibody. The incubation was taken with a secondary antibody conjugated with horseradish peroxidase (HRP) diluted in TBS-T with ratio 1:2000. The procedure was done at room temperature in 1 hour and with gentle agitation. After that, the blot was washed with TBS-T in 5 minutes under agitation thrice to remove residual secondary antibody. The blot is now ready for visualization.

Visualization: The blots were developed with SuperSignal West Femto Chemiluminescent Substrate (Thermo Scientific) according to the manufacturer's instruction. The Image Estimation

2000R (Kodak) was used to visualized the image and the Kodak Molecular Imaging software was used for quantifying band intensity.

Stripping the blot: One blot can be stripped to remove the primary and secondary antibodies from the western blot membrane, so that we can investigate more than one protein on the same blot and save the time, samples and materials. All the steps were done at room temperature with gentle shaking. After visualization, the membrane was incubated twice in an enough volume of mild stripping buffer (appendix 2: Buffers and solutions used in the study) that can cover the membrane for 5-10 minutes each step. The buffer was discarded and the blot was incubated with PBS twice for 10 minutes each step. Finally, the blot was washed twice for 5 minutes each time in TBS-T. The tripped membrane was blocked again by either 5% non-fat milk in TBS-T or 5% bovine serum albumin-fraction V (BSA) in TBS-T in 1 hour under gentle agitation.

3.5.3 Approaches for good western blotting

Samples with viscous cell lysate will result in a bad SDS-PAGE running with smear protein bands. That is because of the DNA in the sample. The DNA should be cut completely by DNAse enzyme, additional nuclease and sonification. Inadequate amounts of lysis buffer also result in too much protein in the sample and the blots run badly. Too much lysis buffer results in too diluted protein and the bands are too faint for detection. It is determined by cell numbers and with MDMs, 150µl of lysis buffer was added over $1x10^6$ cells.

The sample should be quantified by bicinchoninic acid colometric detection, for equal amounts of total loading proteins. However, because the fresh MDMs give out much fat in the lysate and that interferes with the quantification, I could not use this for quantification. I used the 1000 NanoDrop spectrophotometer (Saveen & Werner AB) to measure the overall total protein in lysates. The GAPDH protein was chosen for loading control and reference protein, and the protein intensity values were normalized by GAPDH intensity.

Several factors should be considered, such as whether phosphatase inhibitors should be added to prevent the dephosphorylation and degradation of phospho-proteins, preparation of denatured or native and reduced or non-reduced samples, suitable gel percentage for interesting proteins' molecular weight, control and marker, different blocking reagents are suitable with different antibodies, ratio in dilution of primary and secondary antibodies, blot-stripping methods for different incubation etc.

3.5.4 Antibodies

The western blots were incubated with different antibodies against inflammatory proteins, autophagy LC3B protein, and GAPDH as a reference protein. The diluted factor was optimized by our laboratory researchers previously. Information about these antibodies is included in table 3.2.

Table 3.2. Primary and secondary antibodies for protein assessment by western blotting. (*) is the secondary antibody.

No.	Antibody	Type of Ab	Manufacture No.	Manufacturer
1	TBK1/NAK	Rabbit mAb	#3504	Cell Signaling Technology ®
2	IKKα	Rabbit mAb	#2682	Cell Signaling Technology ®
3	IKKβ	Rabbit mAb	#8943	Cell Signaling Technology ®
4	IKKγ	Rabbit mAb	#2685	Cell Signaling Technology ®
5	IκBα	Rabbit mAb	#4812	Cell Signaling Technology ®
6	NFκB-p65	Rabbit mAb	#8242	Cell Signaling Technology ®
7	IRF3 (FL-425)	Rabbit pAb	Sc-9082	Santa Cruz Biotechnology, Inc.
8	p38 MAPK	Rabbit mAb	#9212	Cell Signaling Technology ®
9	Phospho-TBK1/NAK (Ser172)	Rabbit mAb	#5483	Cell Signaling Technology ®
10	Phospho-IKKα (Ser176)/IKKβ (Ser177)	Rabbit mAb	#2078	Cell Signaling Technology ®
11	Phospho-IKKγ (Ser376)	Rabbit mAb	#2689	Cell Signaling Technology ®
12	Phospho-IκBα (Ser32)	Rabbit mAb	#2859	Cell Signaling Technology ®
13	Phospho-NFκB-p65 (Ser536)	Rabbit mAb	#3033	Cell Signaling Technology ®
14	Phospho-IRF3 (Ser396)	Rabbit pAb	ab138449	Abcam®
15	Phospho-IRF3 (Ser386)	Rabbit mAb	ab76493	Abcam®
16	Phospho-p38 MAPK (Thr180/Tyr182)	Rabbit mAb	#9211S	Cell Signaling Technology ®
17	Keap1	Rabbit pAb	#10503-2-AP	Proteintech™
18	LC3B (D11)	Rabbit mAb	#3868	Cell Signaling Technology ®
19	GAPDH	Mouse	#2118	Abcam®
20	Polyclonal Swine Anti-rabbit Ig/HRP *		P0399	Dako
21	Polyclonal Goat Anti-mouse Ig/HRP *		P0447	Dako

3.6 Optimize the protocol for multiplex real-time Polymerase Chain Reaction (RT-PCR) to quantify Mycobacterial cells per human cell

Most of the pathogenic mycobacterial species have slow growth rates, so that the colony counting method (CFU) is time-consuming, inconvenient and not safe. The quantitative PCR (qPCR) has been developed for quantification of mycobacterial and host DNA in infected human macrophages. CFU counts are routinely used, which has several disadvantages as earlier mentioned, and luciferase assay, which is not stable and depends so much on the batch of bacteria. In addition to my part, I also tried to optimize the protocol from Pathak's paper (Pathak, Awuh, Leversen, Flo, & Asjo, 2012), so that it can be used to quantify mycobacterial cells over human cell in our laboratory.

3.6.1 Basic principles

Polymerase chain reaction (PCR) is firstly used in laboratory technology to amplify millions of copies of specific DNA sequences, instead of using a bacterial system to amplify DNA. As the advantages of this method, it is revolutionized in the field of molecular diagnostics and numbers of applications. One cycle of PCR mainly consists of three steps based on changes of temperature: denaturation at 94-95°c for separation of the complementary DNA strands, annealing step at around 50-60°c for hybridization of the oligonucleotide primers to the template strands, and synthesis step at optimal temperature of DNA polymerase activity for DNA strand elongation. This process continues up to around 40-50 cycles, the exponential phase, after that the amplification rate is decreased due to reagent limitation.

Real-time quantitative PCR (qPCR) is a sensitive, specific, producible and time-saving nucleic acids-quantitative technique. By using probes, dye molecules, amplicons… the proportional amount of nucleic acids is estimated when the accumulating product is immediately detected and measured at each cycle of PCR process. Multiplex real-time qPCR is used to describe the used of many different probes or dyes in one PCR process to detect and measure different templates in a sample. This method saves time, lowering reagent costs, and can control the external and internal nucleic acids (Elnifro, Ashshi, Cooper, & Klapper, 2000).

In this project, we used duplex real-time qPCR with two different TaqMan®MGB probes, FAM and VIC as the fluorescent reporters, and forward and reversed primers for detecting mycobacterial and human DNA in *M. avium* infected MDMs (table 3.3).

Table 3.3: Sequences' information of primers and probes used in duplex real-time qPCR

Detecting species	Name	Sequence
Mycobateria avium - Mycobacterial *65kDa heat-shock protein* gene assay (Myco HSP65)	Primer 1	CGAGGCGATGGACAAGGT
	Primer 2	CTTGTCGAACCGCATACCCT
	Taqman®MGB probe – VIC reporter	AACGAGGGCGTCATCACCGTCG
Human - Human *β-globulin* gene assay (Human BG)	Forward primer	TGCCTATCAGAAAGTGGTGGCT
	Reversed primer	GCTCAAGGCCCTTCATAATATCC
	Taqman®MGB probe – FAM reporter	TGGCTAATGCCCTGGCCCACAA

The hydrolysis probe with reporter at 5' and quencher at 3' will bind to a specific sequence of target gene. The fluorescence will be emitted and detected after the DNA polymerase cleaves the reporter from the probe, as figure 3.5 illustrates.

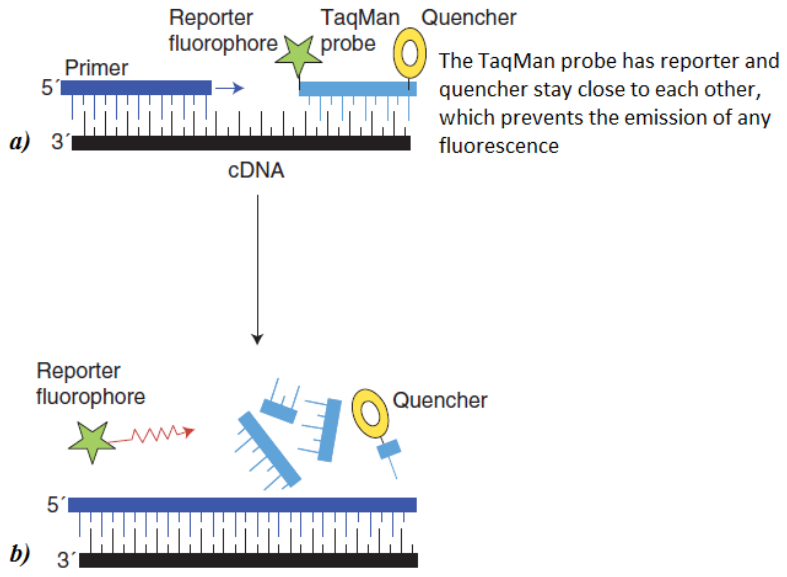

Figure 3.5: Action of TaqMan probe with reporter and quencher. a) Annealing step: The primer and TaqMan probe anneal to the separated DNA strand at specific complementary region. b) Elongation step: The activity of the Taq DNA polymerase cleaves the probe from 5' and separates reporter and quencher dyes. The reporter is disassociated from quencher and emits fluorescence for detection. Taken from (Arya et al., 2005).

3.6.2 Procedure

Sample preparation: The 7-day MDMs cultured in different plates, such as 24-, 48- and 96-well plates, were infected with *M. avium* for 4 hours and then washed with PBS to remove excess mycobacteria. Sterile distilled water was added to each well and incubated for 30 minutes at 37°c to lyse the cell. Matrix tubes were prepared for disruption and homogenization with 0.5g of Precellys 0.1mm glass beads (Bulk bead for 500preps – 0.1mm glass beads, cat no. 03961-1-105) followed autoclaved the tubes. The lysate was collected to one glass-bead containing tube. The well was washed by equal amount of sterile water and collected to the same tube as original lysate to get up to

600µl of solution (detail shown on table 3.4). At this stage, the sample can be stored by frozen at -20 to -80°c.

Table 3.4: Estimated amount of sterile water for different types of plate to get appropriated amount of cell solution for bead-beating

Type of plate	µl of sterile water for first incubation in each well	µl of sterile water for washing in each well	Total µl of solution in glass-bead containg tubes
24-well plate	600	0	600
48-well plate	300	300 x 1 time	600

Disruption and homogenization by FastPrep-24 "bead-beating": Firstly, the *M. avium* was inactivated by heating at 95°c for about 20 minutes, to prevent the spreading of live mycobacteria. Then the samples were cooled down and had bead-beating by FastPrep®-24 instrument (MP Biomedicals). The bead-beating was done 1 time in 45 seconds or 30 seconds with different speeds. The samples were now ready to process qPCR.

Preparation of standard: The DNA stock solutions of *Mycobacterium species* genomic DNA (LGC Standards, VA, USA) and Human Male genomic DNA (Applied Biosystems) were used as standards. The stock concentrations of Myco-standard and Human-standard are 1.97x10^{8} genomes/µl and 3030 genomes/µl, respectively. The dilution was calculated by the estimated number of seeded cells and infected mycobacteria per well.

Quantitative PCR process: The bead-beated samples were tested by qPCR without purification of DNA. The mixture was prepared for each reaction as shown on table 3.5. The QuantiTect® Multiplex PCR Master Mix, myco-primers/probe and human-primers/probe were mixed in a tube and 12µl of mixture was pipetted to each well of MicroAmp® Fast Optical 96-well reaction plate (Applied Biosystems). Then samples and standards were added. The plate was sealed to prevent reagent evaporation, and centrifuged at 1500rpm for 2 minutes to eliminate bubbles. The plate then was loaded into the StepOnePlus PCR machine and used the quantitative – standard curve program followed setting: preheating 95°c for 15 minutes, and 40 cycles of 94°c for 1 minute and 60°c for 1 minute.

The quantitation of samples was calculated by StepOne™ Software version 2.1 (Applied Biosystems), including statistic parameters of each sample. The qPCR was done with duplication to get the best accuracy.

Table 3.5: Volume per reaction mixture for qPCR

Component	Volume needed	Final concentration	Note
QuantiTect® Multiplex PCR Master Mix	10µl	1X	No Uracil-N-Glycosylase (UNG)
Myco-Primers/Probe	1µl	0.4µM of primers	
Human-Primers/Probe	1µl	0.2µM of probe	
DNA templates from standard/sample	8µl	-	Use H_2O in negative control
Total volume per reaction	20µl		

3.7 Statistical analysis

A statistical method was used to analyze the results of different conditions and treatment overall. As least five independent replications were done for each experiment and three to four replications were chosen. The results were put into Excel for organizing and basic calculation. The GraphPad Prism version 6 was used to plot graphic data. The difference between conditions was investigated by using two-tailed student's t-test, with significant difference at p-value < 0.05.

4. Results

4.1 Keap1 negatively regulates inflammatory signaling in *M. avium* infected primary human macrophages

Previous studies have indicated a role of Keap1 in negatively regulating TNF-induced NF-κB signaling through IKKβ degradation and/ or preventing phosphorylation of IKKβ (Kim et al., 2010; Lee et al., 2009). Unpublished results from our group indicate that Keap1 down-regulates inflammatory cytokines during *M. avium* infection (Awuh et al., unbublished). In this present study, we wanted further to investigate the mechanism by which Keap1 regulates inflammatory signaling, and how this may impact intracellular survival of *M. avium* infection in primary human monocyte-derived macrophages (MDMs).

4.1.1 Kinetics of phospho-(p-)IKKα/β and p-NF-κB proteins produced in M. avium infected MDMs

Three experiments were done to examine the amount of inflammatory phospho-proteins at 4 hours post infection. However, we could not detect high levels of phospho-proteins. As phosphorylation of most signal transducing proteins is affected by the time of infection, we next examined MDMs from 1 to 4 hours post infection. Figure 4.1 does not only show that *M. avium* infection activated different inflammatory signaling pathways through inducing phosphorylated proteins, but also show that phosphorylation of IKKα/β and NF-kB were changed dramatically with the time of infection. The amount of p-IKKα/β was high at 1 hour post infection and then gradually decreased with time. p-NF-κB increased and peaked at 1- and 2-hour after infection before it decreased. Meanwhile, p-TBK1 and p-IRF3 were less affected by the time of infection.

Two p-IRF3 antibodies were used: p-IRF3 at Serine (Ser) 396 and at Ser386. The observed results showed 1 band for p-IRF3 (Ser396) at above 49kDa and that was strong in uninfected cells and decreased in infected samples, while p-IRF3 (Ser386) showed 2 bands: one above 49kDa displaying the same trend as p-IRF3 (Ser396), and one below 49kDa with no detection in uninfected sample. These results showed that the *M. avium*-infected macrophages might phosphorylate IRF3 at Ser 386 rather than at Ser 396. The p-IRF3 has three clusters of phosphor-acceptor sites, Ser 385/Ser 386 (cluster I), Ser 396/Ser 398 (cluster II), and Ser 402/Thr 404/Ser 405 (cluster III) (Clément et al.,

2008). The cluster I phosphor-acceptor sites are the most accessible amino acids, and Ser 386 could be the initial target for TBK1/IKKi. While the five serine/threonine residues between 396 and 405 are phosphorylated in response to a viral infection, the Ser-385 and Ser-386 may be specifically phosphorylated in response to induction (UniProt database). Throughout this project, I used the p-IRF3 with phosphorylated group at Serine 386 and the second band for quantification.

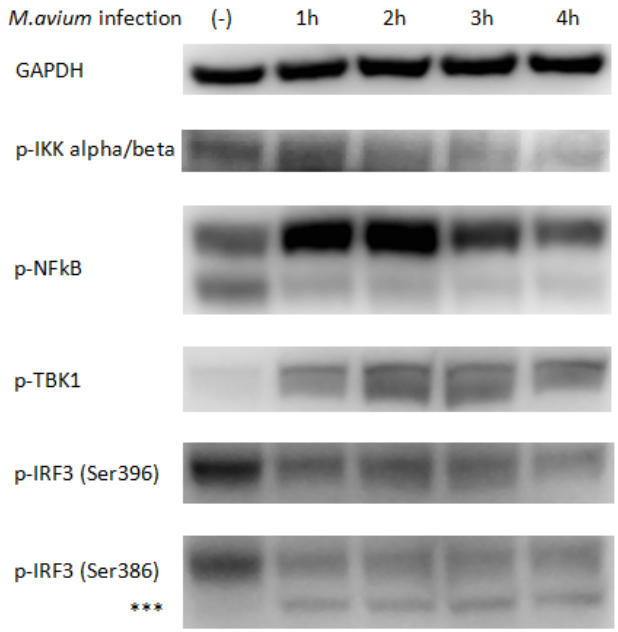

Figure 4.1: Time of infection affects the phosphorylation of inflammatory signaling proteins in *M. avium* infected MDMs. *M. avium* infection was with MOI 10 with no infection as negative control (-). The time interval for infection was 1 hour (1h), 2 hours (2h), 3 hours (3h) and 4 hours (4h) of infection. *** is the lower band at 47kDa of p-IRF3 (Ser386), which is not present in p-IRF3 (Ser396).

4.1.2 Keap1 down regulated the NF-κB signaling pathway through IKK complex during M. avium infection

We knocked down the endogenous Keap1 in human MDMs, and measured the knockdown efficiency by western-blot through induced protein level (figure 4.2). We measured the phosphorylated and total protein levels of 8 different proteins involved in PRR signaling pathways, both NF-κB and type I IFN pathways, and including p38-MAPK (figure 4.3). The measurement was done by immuno-blotting cleared lysate from cells with and without *M. avium* infection. The infection was done with MOI 10 at 30 minutes, 60 minutes and 4 hours after infection.

Ten experiments were done independently and separately, four experiments were chosen for statistical analysis based on healthy cell appearance and high Keap1-knockdown efficiency in all time-points (more than 40% knockdown) (figure 4.2b). Paired student's-test was used to compare the difference between Keap1 siRNA conditions and scramble siRNA control samples, based on the fold induction of protein by infection. The fold induction is the ratio of protein induction in infected samples over uninfected samples after normalization to housekeeping protein GAPDH.

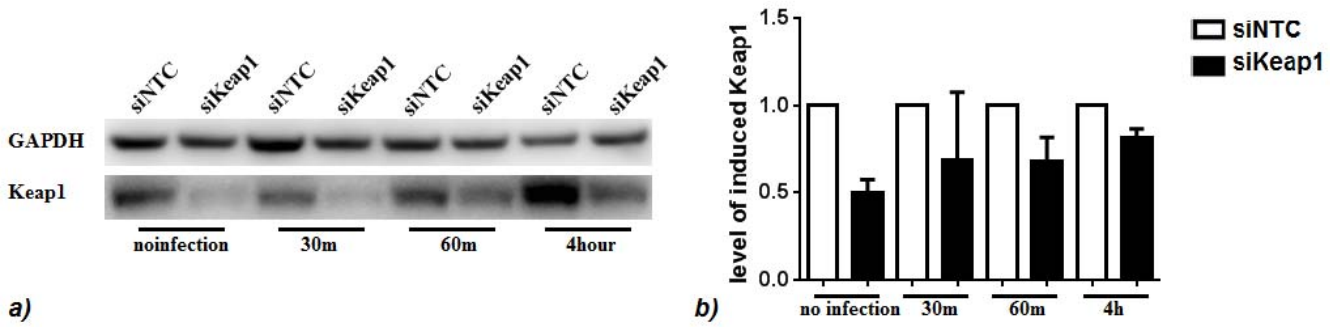

Figure 4.2: Level of Keap1 in siRNA knockdown compared to siNTC sample. a) One representative western-blot used to quantify Keap1 knockdown efficiency. b) The protein level of induced Keap1 in human with Keap1-knockdown sample compared to non-targeted siRNA for negative control (siNTC). The samples were collected from cells with no infection and with *M. avium* infection for 30 minutes (30m), 60 minutes (60m) and 4 hours (4h) with MOI 10. Results from four experiments were graphed with mean and SEM values.

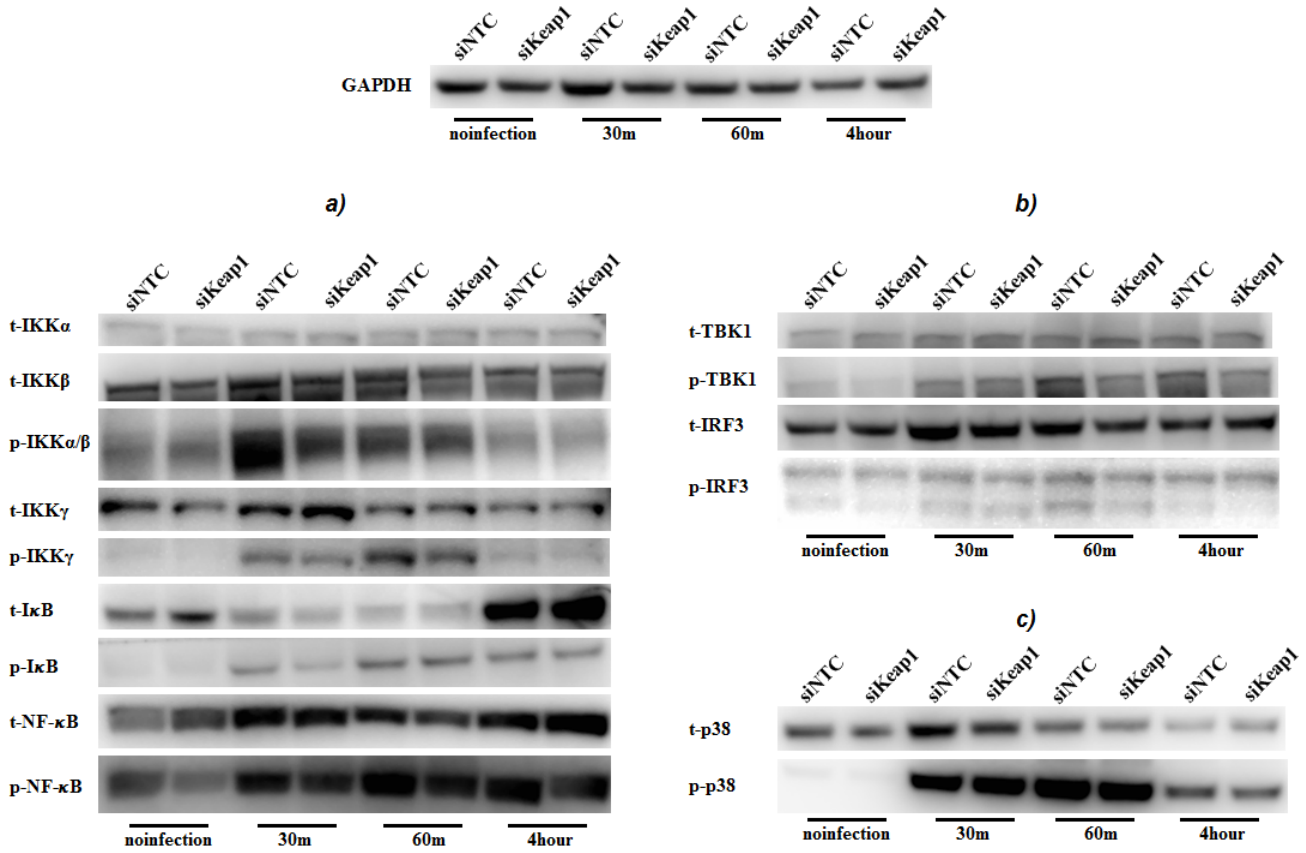

Figure 4.3: One representative western-blot used to quantify level of proteins in three different inflammatory pathways: a) the NF-κB pathway, b) the type I IFN pathway and c) the p-38 MAPK pathway. Here, siKeap1: Keap1-knockdown samples, siNTC: non-targeted siRNA for negative control. The samples were collected from cells with no infection (noinfection) and with *M. avium* infection for 30 minutes (30m), 60 minutes (60m) and 4 hours (4h) with MOI 10.

The IKK complex activation is at the center of the NF-κB signaling pathway. Recent studies have shown that Keap1 down-regulates TNF-induced IKKβ phosphorylation in human cancer cell lines through binding and guiding degradation of IKKβ (Kim et al., 2010; Lee et al., 2009). This is in turn resulted in the down regulation of downstream NF-κB activation as well. In our *M. avium*-infected MDMs, we next investigated if Keap1 regulates phosphorylation and/or total protein levels of the IKK complex (including IKKα, IKKβ, IKKγ), IκB and NF-κB proteins. As figure 4.4 shows, the difference is easily seen in IKK complex and NF-κB in fold induction by infection between negative control and Keap1-knockdown samples, even though the SEM is high between experiments. Knocking down Keap1 significantly increases more than 1.6 factor in t-IKKα and t-IKKγ at 60 minutes and 4 hours of infection, while the increase of t-IKKβ was significant at 60 minutes after infection. Even at 30 minutes and 4 hours after infection, the IKKβ difference is not significant due to high SEM, the high fold induction by infection is easy seen in Keap1 knock-down samples. Both t- and p-NF-κB were significantly higher in Keap1 knock-down samples at 4 hours of infection compared to negative control. When comparing individual experiments, we observed the same trend of protein increase for p-IKKα/β and p-IKKγ in Keap1-knockdown samples, although results were not significant due to high variability between individual experiments. The fold induction of IκB by infection was similar in all time-points with unpredictable trend of changing when comparing individual experiments.

Thus, our results indicate that Keap1 down regulates NF-κB signal through the IKK complex in *M. avium*-infected MDMs.

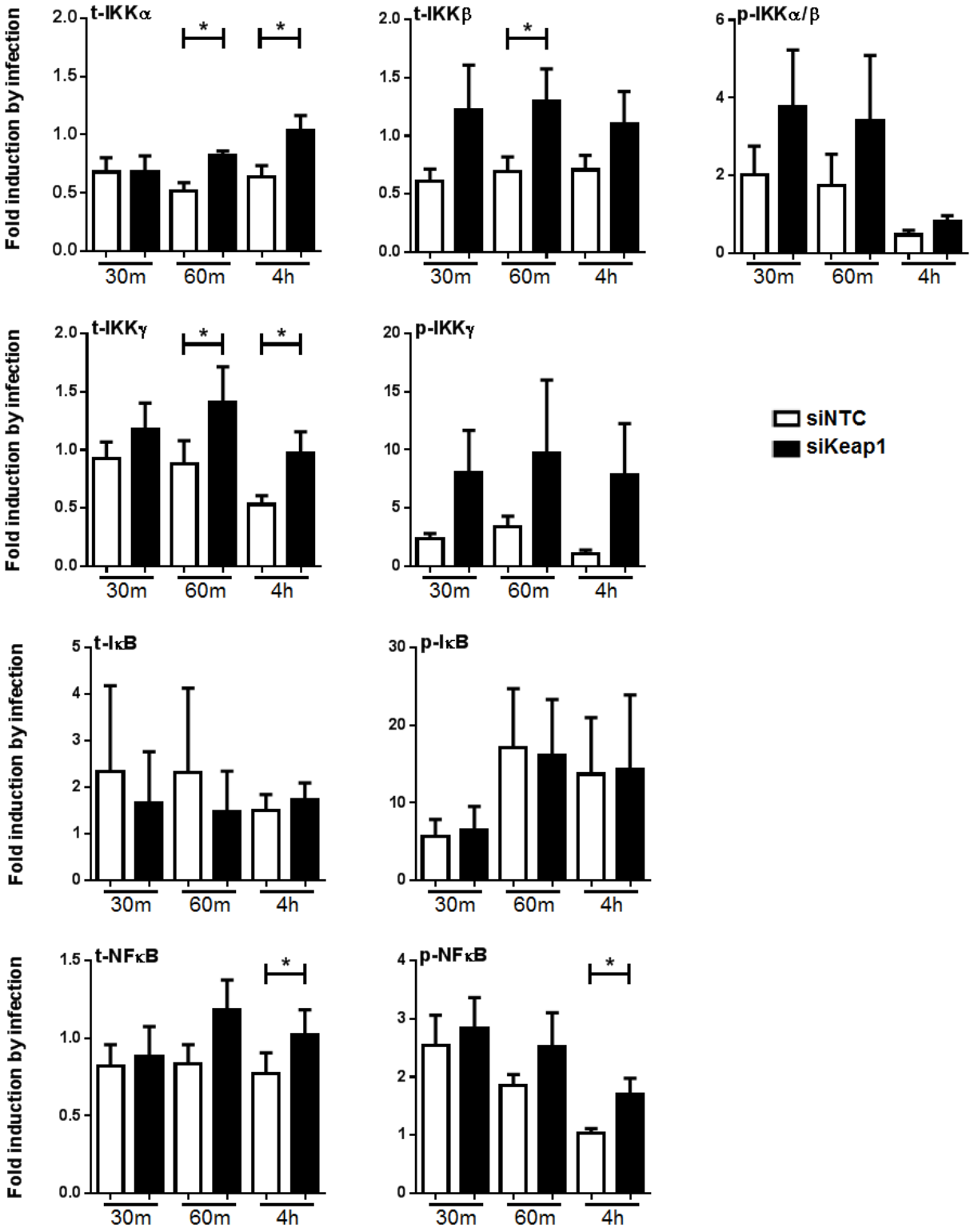

Figure 4.4: Keap1 down regulated the NF-*κ*B signaling pathway through IKK complex during *M. avium* infection. Human MDMs were transfected with siKeap1 for Keap1-knockdown sample (siKeap1) and with non-targeted siRNA for negative control (siNTC). Phosphorylated and total protein levels were examined with antibodies at 30 minutes (30m), 60 minutes (60m) and 4 hours (4h) after *M. avium* infection with MOI 10. Results from four experiments were analyzed by paired student's t-test with p-value<0.05 is significant difference (*).

4.1.3 Keap1 negative regulates TBK1 during M. avium infection

Together with the examination of Keap1's effect on NF-κB signaling pathway, we also did the investigation if Keap1 affects the signaling pathway leading to type I IFN induction. The TBK1 molecule is at the center of the IFN signaling pathway, which commonly phosphorylates IRF3 and IRF7. In our *M. avium*-infected MDMs, we investigated TBK1 and IRF3 proteins. As figure 4.5 shows, both phospho- and total TBK1 are higher in Keap1-knockdown than negative control samples after infection with *M. avium*. However, the difference is significant only with p-TBK1 at 60-minute infection. Meanwhile, with IRF3, we cannot detect any clear difference between two samples. When observing individual experiments, we could see the same trend of increase of both t- and p-TBK1 in Keap1-knockdown samples. The trend of t-IRF3 production was unpredictable with increasing and decreasing between replications; however, the p-IRF3 trend was increasing in Keap1-knockdown samples in three out of four replications with small differences.

This gave evidence that the Keap1 may down regulate TBK1 phosphorylation in *M. avium*-infected MDMs, but the effect on IRF3 is not really known.

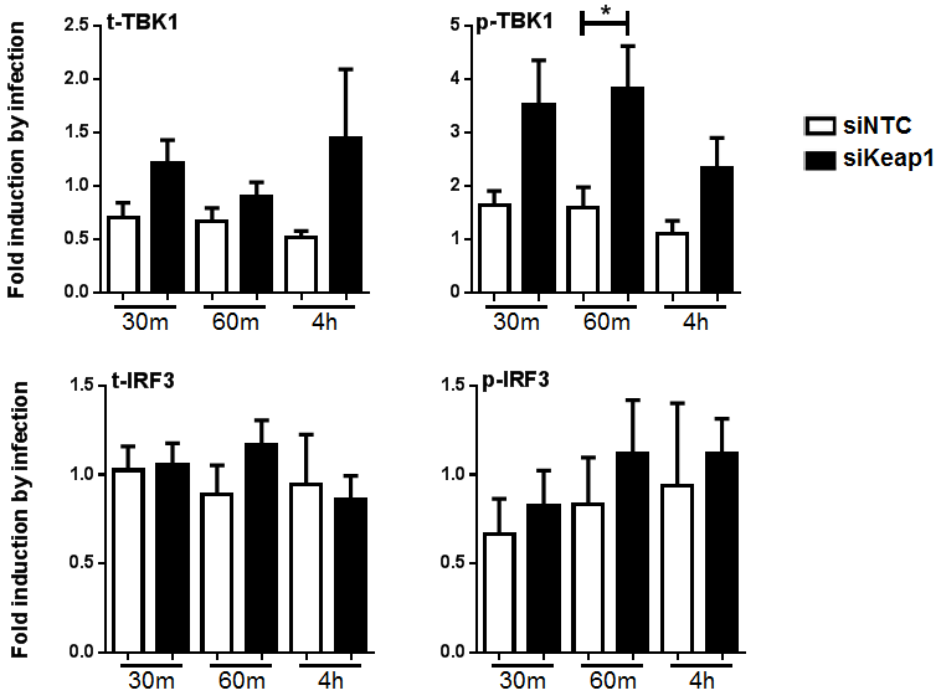

Figure 4.5: Keap1 regulates TBK1 protein in type I IFN signaling pathway during *M. avium* infection. Human MDMs were transfected with siKeap1 for Keap1-knockdown sample (siKeap1) and with non-targeted siRNA for negative control (siNTC). Phosphorylated and total protein levels were examined with antibodies at 30 minutes (30m), 60 minutes (60m) and 4 hours (4h) after *M. avium* infection with MOI 10. Results from four experiments were analyzed by paired student's t-test with *p*-value<0.05 is significant difference (*).

4.1.4 Keap1 has no effect on p38 in MAPK pathway

The MDMs infected with *M. avium* were also examined regarding the effect of Keap1 on the MAPK pathway. One review from Schorey and Cooper stated the role of MAPK as the leader for macrophage signaling upon mycobacterial infection (Schorey & Cooper, 2003). Here, we examined the regulation of p38 as a representative protein in the MAPK pathway that is involved in NF-*κ*B activation and related genes.

With t-p38 induction, the trend was that Keap1 might have an effect on protein levels during the first hour of infection, while at 4-hours infection, t-p38 was up- and down-regulated by Keap1 between different experiments (figure 4.6). It was shown clearly in figure 4.4 even the standard error of the mean (SEM) is high. However, as seen in figure 4.6, the fold induction of p-p38 by infection is not different between negative control and Keap1-knockdown samples. Although in the individual experiment, the difference between Keap1-knockdown and negative control samples could be seen clearly by the high difference in fold induction, the increasing and decreasing trends in protein induction are different between experiment.

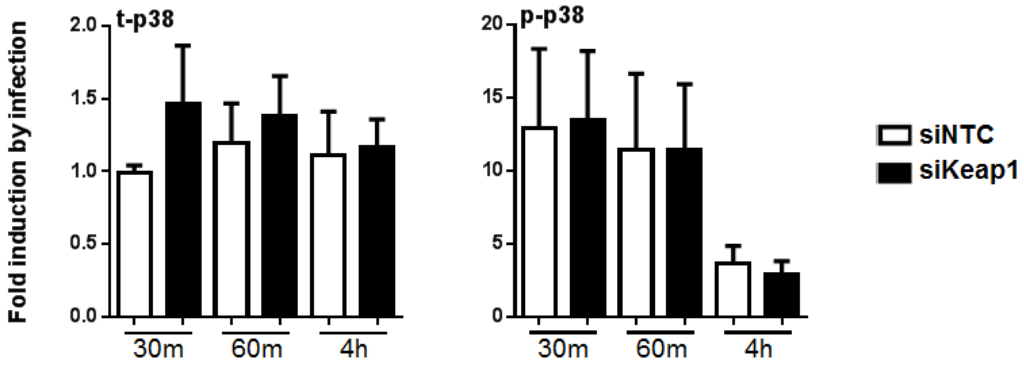

Figure 4.6: Keap1 had no effect on p38-MAPK protein during *M. avium* infection. Human MDMs were transfected with siKeap1 for Keap1-knockdown sample (siKeap1) and with non-targeted siRNA for negative control (siNTC). Phosphorylated and total protein levels were examined with antibody at 30 minutes (30m), 60 minutes (60m) and 4 hours (4h) after *M. avium* infection with MOI 10. Results from four experiments were analyzed by paired student's t-test with *p*-value<0.05 is significant difference (*).

4.2 Keap1 down regulated the autophagy LC3B ii protein in MDMs

Many studies have shown the complex interplay between PRR signaling and autophagy (ref). In addition to binding of Keap1 to Bcl-2, p62 in competition with Nrf2 binds to Keap1 for

degradation by autophagy. Keap1 has binding site with IKKβ and our results suggest that Keap1 plays a role in regulating PRR signaling pathway through IKKs and TBK1. Furthermore, TBK1 is recently shown to be regulating autophagy by promoting autophagic maturation (Pilli, 2012), thus Keaap1 may influence autophagy. Next we investigated if autophagy is affected by Keap1. Our laboratory researchers have found that *M. avium* infection induces autophagy in human macrophages (figure 4.7) (Awuh et al., unbublished). One commonly used marker for autophagy is LC3B ii that is associated with autophagosomal membranes.

To examine the autophagy in MDMs, western blot was used to measure the conversion of cytosolic LC3B i to membrane-associated LC3B ii protein. The *M. avium* infection was done in parallel in both negative non-targeted siRNA control (siNTC) and *Keap1* knock-down (siKeap1) samples with MOI 10. The BAF-A1 was added to the infected samples with a concentration of 100nM 2 hours prior to collecting samples, allowing for accumulation of LC3B ii protein by preventing autophagolysosomal degradation. The time-points for collection of lysates were 4-hour, 24-hour and 72-hour after infection. The immuno-blot of the lysates were incubated with Keap1 antibody for assessing knock-down efficiency at protein level, LC3B antibody for autophagy assessment and GAPDH antibody for loading control and reference.

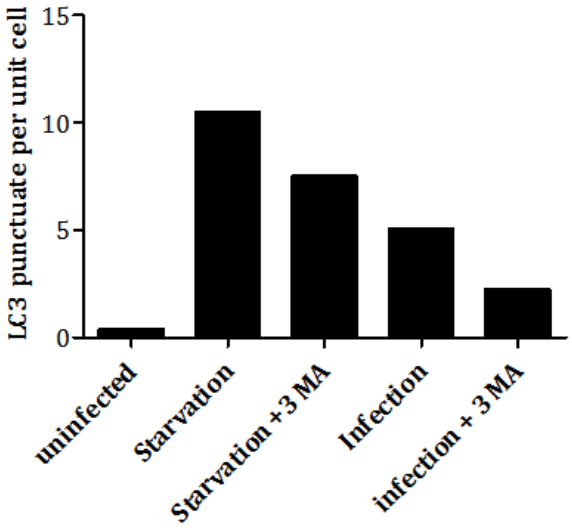

Figure 4.7: *M. avium* infection induces autophagy in primary human macrophage. The human primary macrophage were either infected with CFP- *M .avium* for 4 hours, amino acid starved in Hanks balanced salt solution or amino acid starved in presence of 3MA for 2 hours. To elucidate the basal autophagy, cells with no treatment was also included in the study. All the conditioned samples were treated with 100nM of BAF-A1 in 2 hours prior analysis. The experiment was done by counting LC3B ii dots under confocal microscopy. (with permission from Shrestha, Birendra K.)

Six experiments were done independently and separately giving different levels of *Keap1* knockdown. The knockdown efficiency was different between experiments and between wells in one plate. We eliminated the experiments that had low knockdown efficiency and highly uneven knockdown between time-points. Among them, three experiments were chosen which had highest knockdown efficiency (more than 20%) in all time-points for statistic analysis (figure 4.9a). The

effect of Keap1 on produced LC3B ii protein was investigated by unpaired student's t-test on fold induction of LC3B ii protein in Keap1-knockdown sample over control sample at each time-point.

As shown in figure 4.8, the LC3B proteins gave 2 bands with different molecular sizes after LC3B-antibody incubation. They are cytosolic LC3B i (16kDa) and autophagosomal LC3B ii (14kDa). When autophagy processes, the cytosolic LC3i will conjugate to phosphatidylethanolamine to form autophagosomal LC3ii for inserting to the phagophore membrane. From the immuno-blot, the GAPDH is not equal in every sample, so that we could not interpret accurately the result by comparing bands. The intensity of bands was measured to normalize over GAPDH for trusted values.

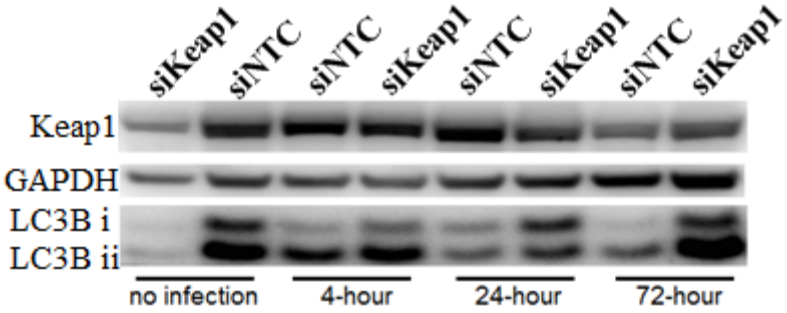

Figure 4.8: One representive western-blot used to quantify Keap1 and LC3B protein. Here, siKeap1: Keap1-knockdown, siNTC: non-targeted siRNA transfection as negative control, 4-hour: 4 hours after infection, 24-hour: 24 hours after infection, and 72-hour: 72 hours after infection.

To do the comparative effectiveness of Keap1 on LC3B ii induction, we made a relative value of normalized intensity of LC3B ii by GAPDH between siKeap1 samples over siNTC samples at each time-point. That means all the LC3B ii values in negative control are 1 (represented for 100%) for a control and basic level of LC3B ii induction in both uninfected and infected MDMs. Statistic unpaired student's t-test method was used to evaluate the significant difference between two siRNA conditions at each time-point. Figure 4.9b) shows the higher amount of LC3B ii protein in all infection time-points in Keap1-knockdown samples comparing to negative control samples. The difference is significant at 24 hours after infection. The SEM of LC3B ii formation at no infection and 72-hour infection are relatively large, due to the uneven knockdown efficiency between wells and between donors of MDMs. Additionally, when we did the knockdown, the reagents from the siRNA transfection may induce autophagy within cells even though there was no infection (ref). This is also the reason why the LC3ii formation is so different in samples at no infection time point. And the ineffectiveness of siRNA transfection after a long time gave variety in results.

The experiments showed that Keap1 down regulates the formation of autophagosomal LC3B ii in *M. avium*-infected MDMs at least throughout of first day of infection.

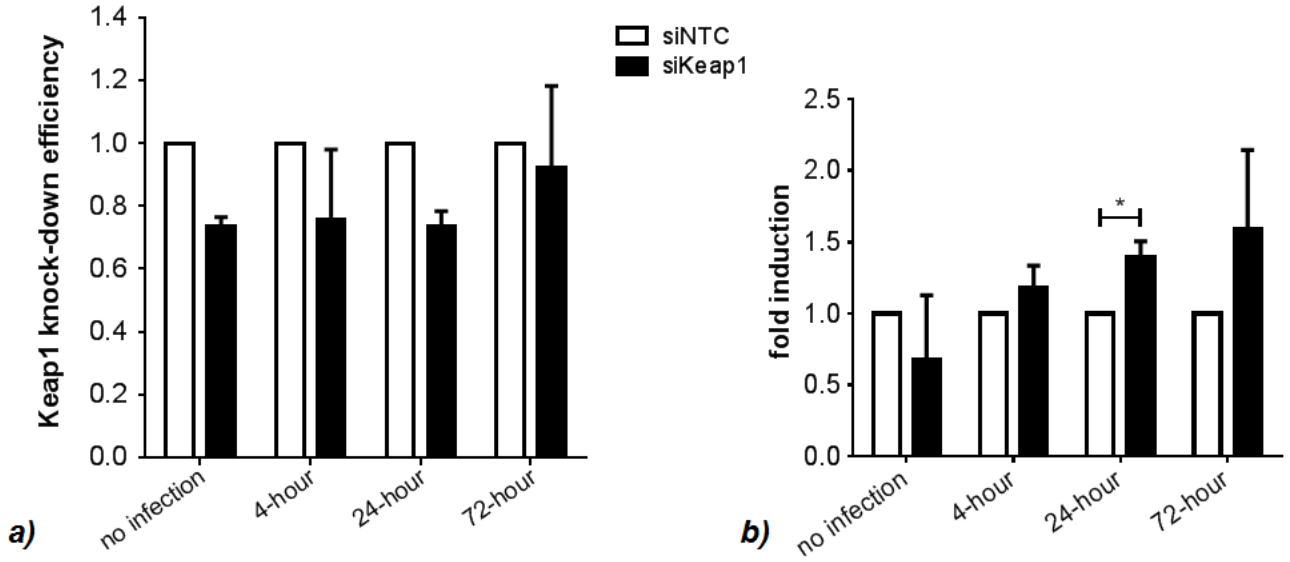

Figure 4.9: Effect of Keap1 on LC3B ii induction by immuno-blot method. a) Keap1-knockdown efficiency of siRNA Keap1 transfection samples compared to non targeted siRNA transfection at each time-point in MDMs. b) Keap1-knockdown MDMs had higher induction of LC3B ii protein compared to negative control siNTC MDMs and it is significantly different at 24-hour infection. Unpaired student's t-test method was used to compare relative values with significant difference at p-value < 0.05 (*). Here, siKeap1: samples with siRNA *Keap1* transfection, siNTC: samples with non-targeted siRNA transfection/negative control, 4-hour: 4 hours after infection, 24-hour: 24 hours after infection, and 72-hour: 72 hours after infection. The values represent mean and standard error of the mean (SEM) between 3 experiments.

The conclusion from the western-blot that autophagy may be affected by Keap1 was supported by results from the confocal experiments, which was done by Birendra K. Shrestha. The Keap1 knock-down efficiency was accessed by real-time PCR of Keap1 mRNA in cells. He did count the formation of LC3ii dots with the same time-points of infection. LC3B ii is lipidated and punctuated on the membranes of autophagosomes, which appears as a dot in fluorescence microscopy in contrast to the diffuse cytosolic form of LC3B i. Figure 4.10 also show the increase in autophagosomal LC3B in Keap1-knockdown comparing to negative control samples. The difference is also significant at 24-hour infection.

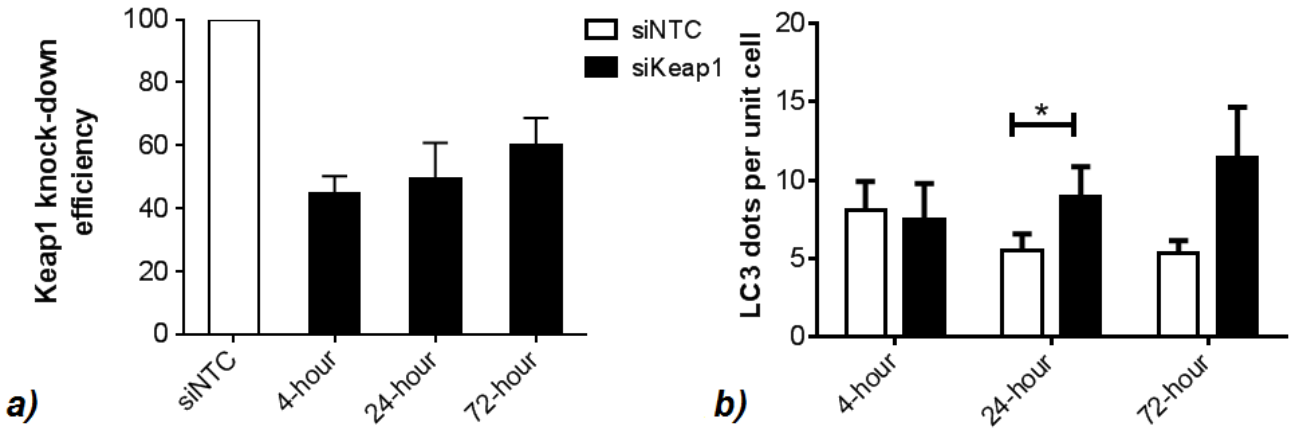

Figure 4.10: Effect of Keap1 on LC3B ii induction by confocal microscopy method. a) Keap1 knock-down efficiency assessing by real-time PCR at mRNA level. b) LC3-dot formation was higher in Keap1-knockdown sample than in negative control samples and significantly different at 24-hour infection. Unpaired student's t-test method was used to compare relative values with significant difference at *p*-value < 0.05 (*). Here, siKeap1: samples with siRNA *Keap1* transfection, siNTC: samples with non-targeted siRNA transfection/negative control, 4-hour: 4 hours after infection, 24-hour: 24 hours after infection, and 72-hour: 72 hours after infection. The values represent mean and standard error of the mean (SEM) between 3 experiments. (with permission from Shrestha, Birendra K.)

4.3 Keap1 affects the survival of intracellular *M. avium* in MDMs

In every bacterial and viral infection, both inflammatory cytokines and autophagy play important roles in control the survival and growth of pathogens. We found an effect of Keap1 on inflammatory pathways and autophagy in *M. avium* infected MDMs. That is the reason why we investigated the survival of intracellular mycobacteria in MDMs, so if it is affected by Keap1.

Keap1 gene was knockdown by siRNA transfection and negative control was made by transfection of non targeted siRNA. *M. avium* expressing luciferase was used to infect with MOI 10. The samples were collected at three different time points, lysed and incubated with D-luciferin in 5 minutes to measure the luciferase activity. The luciferase activity is used to represent the amount of intracellular *M. avium* expressing luciferase in infected MDMs. The t-test was done to compare the difference between negative control and *Keap1*-knockdown samples at each time point of infection.

As shown in figure 4.11, at 4 hours post infection, equal value of luciferase activity showed equal uptake of *M. avium* by MDMs. After 24 hours of infection, bacterial numbers in Keap1-knockdown samples were slightly lower than in the negative control. And in the 72-hour infection, the difference in the number of intracellular *M. avium* between siKeap1 and siNTC samples was

clearly observed. It was repeated in 3 independent experiments. It indicated that in the Keap1-knockdown samples, the survival and growth of intracellular *M. avium* was restricted compared to control samples, although the difference was not significant.

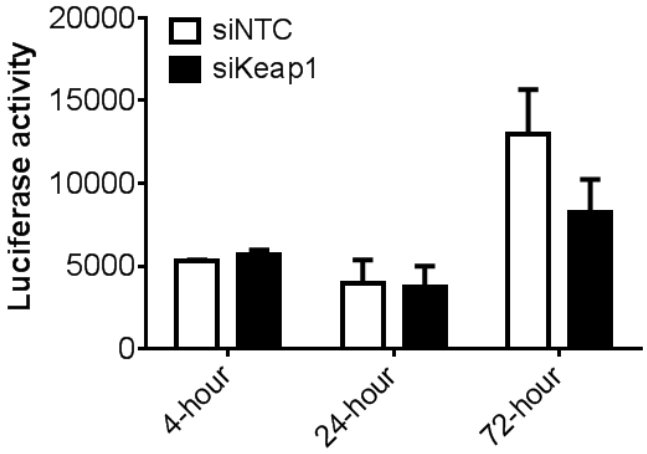

Figure 4.11: The growth of intracellular *M. avium* might be affected by Keap1. At 4-hour and 24-hour infection, the difference between siNTC and siKeap1 samples is not much with approximately equal number of bacteria. While at 72-hour infection, the growth of *M. avium* was slower in *Keap1*-knockdown than in negative control samples, however, the difference is not significant (p-value > 0.05). Here, siKeap1: samples with siRNA *Keap1* transfection, siNTC: samples with non-targeted siRNA transfection/negative control, 4-hour: 4 hours after infection, 24-hour: 24 hours after infection, and 72-hour: 72 hours after infection. The values represent mean and standard error of the mean (SEM) between 3 experiments.

4.4 Quantitation of Mycobaterial cells per human cell by PCR

When doing mycobacterial survival experiment, we encountered problems with the quantification method that we used. Both CFU and luciferase assay can not quantify the number of human cells in one well, which also has an effect on the number of intracellular mycobacteria. The routine CFU method is time-consuming as it requires up to 10 days for countable colonies, not safe and not correct as the formation of aggregates might underestimate the number of bacteria. As the same with luciferase assay, the quality of result depends so much on the batch of infected bacteria, such as health, time of culture and quality of substrate and lysis buffer. Both quantification methods meet the same problem that the number of cells in different wells can not be quantified. Each well in the same plate might have different quality and it also affected the growth and survival of the human cells. That caused slightly different number of cells in different wells, in which we had different

conditions of treatment. In addition, through the long time of infection, some cells will die and some will survive with different proportions, and this causes problems in the exact quantification of the number of intracellular mycobacteria. That is the reason why we tried to use the multiplex real-time PCR to quantify the mycobacterial cells per human cells.

When trying to follow the protocol from Pathak *et al.*'s paper, we found out that our bead-beating system had different parameters of speeds (Pathak et al., 2012). So when trying the maximum speed of the FastPrep-24 system in 45 seconds, we could not detect any reliable results from both human cells and mycobacterial cells. We hypothesized that our glass beads together with high speed may be destroy the DNA. So, we established a screening in both time and speeds. These are six different speeds from 4.0m/s to 6.5m/s with 0.5m/s increase for each condition, and bead-beating 1 time in 30 seconds or 45 seconds. The results are summarized in figure 4.12 from one experiment with duplication in both biology and technique. The infection was done in 4 hours with MOI 10 of *M. avium* per MDM. After 4 hours of infection, the samples were washed to remove any excess mycobacteria on the surface of cells. Experiments were done in a 48-well plate, so by estimation, there should be 125,000 human cells and 12.5×10^5 mycobacterial cells in each well. We could see that bead-beating in 45 seconds gave the most accurate number of both human and mycobacterial cells. Among them, speeds of 5.5m/s and 6.0m/s gave the best accuracy and similar results.

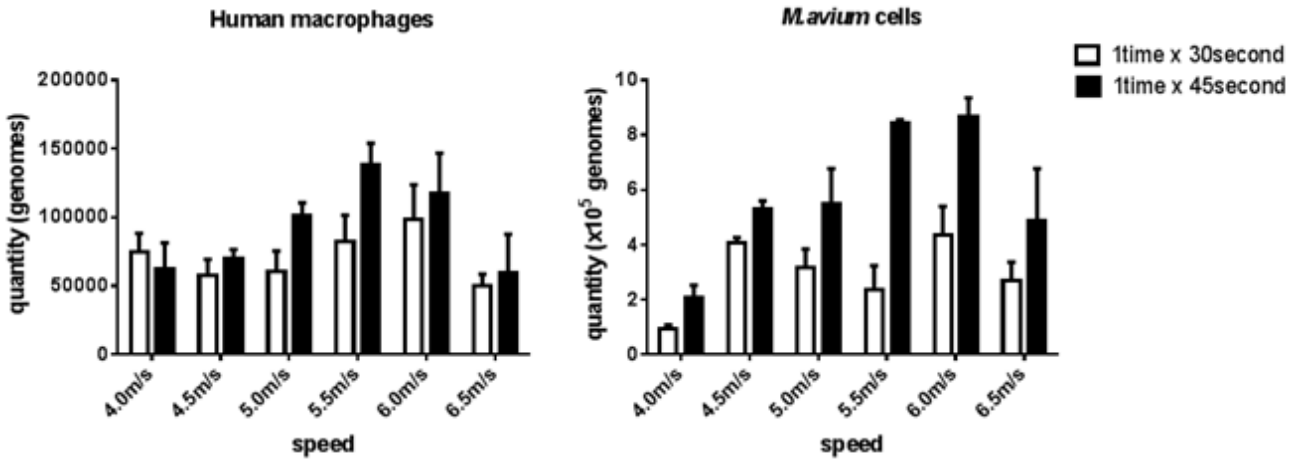

Figure 4.12: Screening for the detected amount of human and mycobacterial cells by duplex PCR. The results were summarized from one experiment with duplication in both biology and technique. The infection was done in 4 hours with MOI 10 of *M. avium* in 48-well plate.

The mycobacterial result was also quantified by CFU. The colonies were calculated and made into log numbers to compare with qPCR results. As shown by figure 4.13, that the number of mycobacterial cells detected by qPCR was higher than the number of counted colonies by CFU,

confirming the results in the paper by Pathak *et al.* (Pathak et al., 2012). This was explained by causing of bacterial aggregation, dead and live cells; that because the qPCR can not discriminate DNA from dead cells and live cells. So it is necessary for many replications to make a relationship between CFU counts and qPCR detection. Because each different laboratory has different reagents and equipment, the related equations may be different between laboratories and set up.

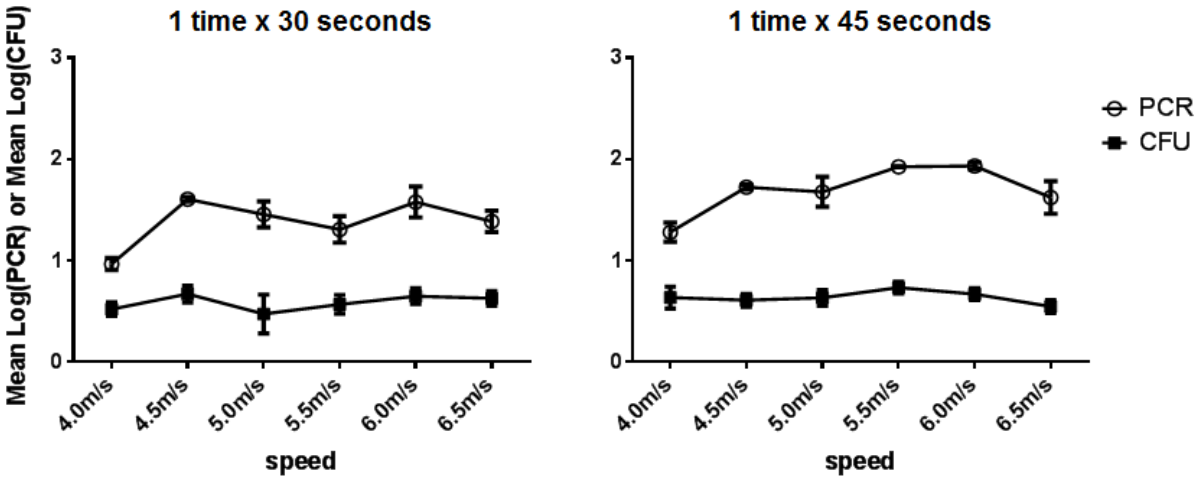

Figure 4.13: Mycobacterial cells in infected human macrophages as measured by colony counting (CFU) and qPCR (PCR). The results were summarized from one experiment with duplication in both biology and technique. The infection was done in 4 hours with MOI of *M. avium* 10 in 48-well plate.

5. Discussion

The overall aim of this project was to investigate the role of Keap1 in mycobacterial infection, especially *M. avium*. Keap1 acts as the cellular sensor for oxidative stresses (H. K. Bryan et al., 2013; Ogura et al., 2010). It is an inhibitor protein of Nrf2, is a substrate adaptor of a Cul3-based E3 ubiquitin ligase complex that recognizes, binds, and ubiquitinates Nrf2 and guides it for proteasome degradation. We hypothesized that the Keap1 may have a negative effect in controlling the *M. avium* infection. Through its binding to IKKβ, an important signaling protein in the innate immune system, Keap1 guides IKKβ for degradation thus prevents the phosphorylation of IKKβ in inflammatory pathways. The first inflammatory responses are affected and cause disadvantage in initiating the whole immune system responses. Thus, in this study, we knocked down the *Keap1* gene in cells for preliminary observation. With the suggestion by Lee *et al.*, functions mediated by Keap1 may be varied from small to large animals due to genetic differences; hence we used primary human MDMs in this study (Lee et al., 2009). In addition, human macrophages are the most relevant cell type in mycobacterial infection. These preliminary observations are suggestive of a new role of Keap1 in the control of mycobacterial infection.

With initial observation from the measurement of both NF-*κ*B and IRF regulated cytokines, it was shown that Keap1 does not only regulate the NF-*κ*B response shown in previous studies, but also regulates the type I IFN response in inflammation resulting from *M. avium* infection. It was shown through the down regulation of the expression of the IL-6, TNF-α, IL-1β, type I IFN, IFN-β and IP-10 in both ELISA and real-time PCR measurement. Several studies have shown the importance of the type I IFN response to the bacterial infection, in addition to its antiviral activity, including *Escheriachia coli* and *M.tuberculosis* (Husebye et al., 2010; Pandey et al., 2009; Wu et al., 2010).

The first and most important finding in our studies is the control of Keap1 to TBK1 in *M. avium*-infected MDMs. There is no studies or researches that shows the relation or interaction between TBK1 and Keap1. And we found that both the total and phosphorylated TBK1 is increased in Keap1-knockdown MDMs. In theory, TBK1 is the central protein of type I IFN pathways and phosphorylated TBK1 leads to the activation of IRF3, one of the transcription factor for type I IFN. However, we could not detect any clear difference in IRF3 between Keap1-knockdown and negative control samples. While the cytokine experiments showed the difference in induced IFN, we believed that other IRF, such as IRF7 or IRF5, may be involved in MDMs during *M. avium* infection. But, we

have not examined more in other IRF due to lack of antibodies. Moreover, TBK1 also provides many roles in different layers of immunity. Not only involved in type I IFN pathways, but TBK1 also have shown that it is a kinase that activates NF-*κ*B pathway and it is a mediator that positively regulates autophagy. That will be discussed later.

In the NF-κB signaling pathway, the subunits of the IKK complex work together to trigger IκB phosphorylation and proteasomal degradation, releasing active transcriptional factor NF-κB. With two different NF-*κ*B pathways, the components of the complex, IKKα, IKKβ and IKKγ, are likely to be regulated by different factors and under particular conditions (Ramakrishnan et al., 2004). Our results clearly indicate a role of Keap1 in NF-*κ*B pathway through controlling the expression of IKK complex. Together with the total proteins was increase in Keap1-knockdown sample, the phosphorylated IKK complex in Keap1-knockdown samples was higher than in negative control. While recent studies have only showed that Keap1 down-regulates the IKKβ phosphorylation through binding and guiding degradation of IKKβ (Kim et al., 2010; Lee et al., 2009), we observed the negative regulation of Keap1 in all IKK molecules. In the experiments of Lee and colleague, they also showed the upregulation of IKKγ in Keap1-knockdown sample, but they did not go deep into that protein (Lee et al., 2009).The IKKβ was investigated in detail and they discovered the E(T/S)GE binding site on this IKKβ to Keap1, while IKKγ protein sequence does not have that domain. Same with IKKα, even IKKα and IKKβ have similar genetic structure with 50.1% identity and 67.1% similarity in amino acid (Sequence Manipulation Suite: Pairwise Align Protein), it does not contain E(T/S)GE binding site for Keap1. And thus Kim and others did not make the observation on IKKα (Kim et al., 2010). However, our results showed evidence that IKKα is also under the effect of Keap1 during *M. avium* infection in MDMs.

Genetic experiments have shown that IKKβ is the predominant IκB kinase, relative to IKKα (Pasparakis, Luedde, & Schmidt-Supprian, 2006), both Lee *et al.* and our studies supported the finding of Ramakrishnan *et al.* that the phosphorylation of I*κ*B is dependent on IKKβ and IKKγ in a classical pathway (Ramakrishnan et al., 2004). And somehow Keap1 might have role in IKKγ induction also. In both studies of Lee *et al.* and Kim *et al.*, they showed that IKKα was not down-regulated by Keap1, and supported their hypothesis that IKKα does not have the binding target motif and did not interact with Keap1 (Kim et al., 2010; Lee et al., 2009). However, we detected the significant difference in IKKα induction between Keap1-knockdown and negative control samples, especially at 4-hour infection. Because IKKα does not have the E(T/S)GE binding site for direct interaction with Keap1, we anticipated that the IKKα was indirectly under the effect of Keap1 which

directly affects production of IKKβ and may also affects IKKγ directly or undirectly. It was mentioned early that the activation of IKKα is characterized as the alternative NF-κB pathway and IKKα is activated through TNF cytokines family, but not TNF-α (Ramakrishnan et al., 2004). Moreover, we observed that the increase of IKKα induction was smaller and later than the increase of IKKβ and IKKγ in Keap1-knockdown samples. Thus, the increase of total IKKα in Keap1-knockdown could be the result of the effect of Keap1-knockdown in cytokine production. In Tamura *et al.*'s review, IKKα waas shown that it may have role in type I IFN pathway, especially it may activate IRF7. It supports more for our above discussion about the result of IRF3. Thus, we may need to examine the changing of protein level of other IRF molecules in Keap1-knockdown samples.

With all the increase of IKK complex molecules by Keap1-knockdown, this is in turn shows the down regulation of downstream NF-κB activation as well in our results, the difference is significant in both total and phosphorylated NF-κB at 4 hours after infection with high level in Keap1-knockdown samples. It has shown that NF-κB has both classical and alternative pathways which are activated via different phosphorylated IKKβ and IKKα (Ramakrishnan, 2004). While IKKβ is mainly phosphorylated by ligands triggering, IKKα is activated by TNF family cytokines. It is proposed the second phase response of NF-κB via IKKα after a certain time of infection. This evidence gave more support to the role of Keap1 in both initial infection and loop period in IKK complex and NF-κB difference. When observing IκB protein level, we saw that fold induction of phosphorylated IκB by infection was similar in all time-points between Keap1-knockdown and negative control samples. It can be explained that the IκB after being phosphorylated by phospho-IKK complex will be directed to degradation. That caused the difficulty in measuring the actual amount of IκB protein, which is degraded after phosphorylated in cells. In addition, under particular conditions, TBK1 is reported to have a function as an NF-κB effector by phosphorylating related proteins for NF-κB translocation (Tojima et al., 2000; Viatour, Merville, Bours, & Chariot, 2005). Further, this suggests that Keap1 might negatively control the activation of PRR-induced inflammatory signaling, not only through the IKK complex but also through TBK1. This leads to another layer on the regulation of TBK1 and its downstream effectors.

In summary, we observed that the Keap1-knockdown MDMs with *M. aium* infection have upregulated both IKK complex and TBK1. But only IKKβ has the ETGE binding site with Keap1, which leads to the degradation of IKKβ by ubiquitinase proteins (Kim et al., 2010; Lee et al., 2009). Thus, Keap1 leads to the prevention of phosphorylating IKKβ for activation. While IKKα, IKKγ and TBK1 do not have EGTE binding site with Keap1, it is believed that Keap1 might have indirect

interaction with these proteins or they might have different binding site. As explained previously, IKKα is reported to be activated though TNF cytokines family (not TNF-α), so that Keap1 has an indirect negative effect to IKKα through the feedback of inflammatory cytokines. With IKKγ and TBK1, there is no study about the effect or the binding site of these proteins with Keap1. Our results support the evidence that Keap1 has control in both IKKγ and TBK1. However, the mechanism of interaction is still unclear. Both total and phospho-IKKγ are affected by Keap1, theorily, the effect could be the results of the transcriptional process, the protein synthesis, the binding leading to degradation of proteins, the prevention of phosphorylation or the degradation of phosphoprotein. It is the same with TBK1, there is little knowledge about TBK1 and Keap1 interaction. It is needed to investigate the mechanism more in detail. Together, our observation and these data indicate that Keap1 regulation might have broad consequences in the innate immune response to mycobacterial infection at initial infection and also loop feedback.

In addition to PRR signaling, there is much research stating the link between p62, which is selective substrate for autophagy, and Keap1 (Bjorkoy et al., 2005; Jain et al., 2010; Komatsu et al., 2010). p62 directly interacts with LC3 and then regulates the formation of autophagy. p62 also has direct interaction with Keap1 for targeting degradation, then therefore will stabilize the ROS transcription factor Nrf2. Fan and colleagues' studies about Keap1 and p62 and also Stepkowski and Kruszewski's hypothesis about Keap1 and its interplay showed the bridge of p62 between Keap1 and ubiquitin aggregates in autophagy (Fan et al., 2010; Stepkowski & Kruszewski, 2011). Also, many studies implicate the function of TBK1 as mediation of autophagy. Bacterial proliferation is restricted by TBK1 through phosphorylating the autophagy receptor Optineurin (OPTN), thus it increases the LC3 binding affinity and antibacterial autophagy (Pilli et al., 2012; Thurston, Ryzhakov, Bloor, von Muhlinnen, & Randow, 2009). Moreover, Keap1 is shown by Niture and Jaiswal that to target Bcl-2 for degradation, while Bcl-2 belongs to protein family that regulates both apoptosis and autophagy (Levine et al., 2008). A recent study of Watson *et al.* showed that Mtb induced autophagy independent of inducers (Watson, Manzanillo, & Cox, 2012). Our laboratory researchers also found that *M. avium* infection induces autophagy and it is regulated by Keap1 (Awuh et al., unbublished). In the present study, we found that there was a higher amount of LC3B ii protein in all infection time-points in Keap1-knockdown samples compared to negative control samples in immuno-blotting method, but it is not in the confocal microscopy experiment. In confocal experiment, the LC3B ii accumulation was decreased by Keap1 knockdown at 4-hour infection. These findings are in line with a study describing the role of Keap1 in the positive regulation of autophagy (Fan et al., 2010).

However, in both quantification methods, the LC3B ii accumulation did tend to increase in Keap1-knockdown at 24-hour and 72-hour of infection. This suggests that at the later stage of infection, the autophagy is negatively regulated by Keap1. Together, these observations show that autophagy can be induced by *M. avium* and that Keap1 may play an important role in regulating mycobacterial autophagy.

Given the role in regulation of Keap1 in both inflammatory and autophagic pathways, we continued to investigate whether the Keap1 knockdown influenced the survival and growth of intracellular mycobacteria in MDMs. We showed that after 3 days of infection, the difference in bacterial numbers was clearly shown. The mechanism behind this appears complex but may be explained. We observed that the inflammatory cytokines were upregulated during first 4 hours of infection and the LC3B ii protein-related autophagy seemed to be increased at 24-hour of infection in Keap1-knockdown samples. This indicated that the Keap1 may play a critical role in the early stage in host response to infection, and that it plays an important role in deciding the outcome of later responses of the host to infection. However, we don't know if the restrict in number of mycobacteria by Keap1-knockdown is the result of inhibiting growth or killing cells. In addition, there is evidence which showed that autophagy has dual roles in *M.tb* infection: antibacterial and anti-inflammatory properties (Castillo et al., 2012). Perhaps, the autophagy also may be induced to protect the host from damage caused by inflammation. Together, the role of Keap1 in controlling inflammatory response is shown, and also its role in regulating autophagy for bacterial killing. Thus, Keap1 acts as a cytosolic sensor and an interplay factor of the innate immune system, at the crossroads of ROS generation, inflammatory and autophagy that restrict the growth of intracellular *M. avium* in human macrophages.

Our studies were done *in vitro* with primary human macrophages, which are very hard for isolation and culturing. The healthy status of macrophages is also different from donor to donor, that gives the unstable in controlling the cell culture. The unstable and difference of MDMs cause the high error between experiments when we did the statistical analysis. In addition, our siRNA transfection system is not very effective. The knockdown efficiency is different between well to well on the same plate, and between donor to donor. Even the PRC analysis gave out the result with high knockdown in mRNA level, the knockdown efficiency in protein level is different and still low. Moreover, the transfected reagents are seemed to hard for primary macrophages that sometimes caused cell death. And the scramble siRNA for negative control gave out background responses, that causes difficulty for analyzing the difference. It is very important to find out another solution for the knockdown system.

6. Conclusions and future perspectives

Keap1 might have a role as a link between ROS, inflammation and autophagy that is very important in controlling *M. avium* infection at early responses. With the overall aim of investigating the immune response mechanism and killing of *M. avium* in human primary macrophages, Keap1 was knocked down to examine the role in regulating different proteins in both inflammatory and autophagy pathways, especially in primary human monocyte-derived macrophages (MDMs).

Our results show the role of Keap1 in down regulating both the central IKK complex and TBK1 proteins in inflammatory pathway, followed by the down regulation of the transcription factor NF-κB. However, at the time we did not have the reagents and equipment to examine other IRF molecules than IRF3 but this work is in progress. In autophagy, Keap1 makes a difference with Bcl-2 hypothesis, that Keap1-knockdown samples had higher induced autophagy than the negative control. Our observation was supported by the increase of TBK1 by Keap1 knockdown together with the requirement of TBK1 for autophagic maturation. Those together make sense on the controlling of intracellular mycobacterial *M. avium* in MDMs, that the number of bacteria in Keap1-knockdown is less than in negative control.

In summary, our results gave that although with Keap1 presents in MDMs, both the inflammatory response and autophagy were less than in MDMs with Keap1-knockdown. Together with the decrease of intracellular bacterial numbers in Keap1-knockdown MDMs, it does not necessarily mean that the Keap1 gives disadvantage in controlling the *M. avium* infection. Our study was done *in vitro* and limited to the macrophages only. We suggest looking at the role of Keap1 in the adaptive immune system to see clearly the effect of Keap1 in whole system.

References

Abdallah, A. M., van Pittius, N. C. G., Champion, P. A. D., Cox, J. S., Luirink, J., Vandenbroucke_Grauls, C. M. J. E., . . . Bitter, W. (2007). Type VII secretion - mycobacteria show the way. *Nature reviews microbiology, 5*, 9.

Aderem, A., & Underhill, D. M. (1999). Mechanisms of phagocytosis in macrophages. *Annual review of Immunology, 17*, 31.

Appelberg, R. (2006). Pathogenesis of *Mycobacterium aivum* infection. Typical response to an atypical mycobacterium? *Immunologic research, 35*, 12.

Arya, M., Shergill, I. S., Williamson, M., Gommersall, L., Arya, N., & Patel, H. R. H. (2005). Basic principles of real-time quantitative PCR. *Expert Review in Molecular Diagnostics, 5*, 11.

Awuh, J. A., Haug, M., Marstad, A., Do, C. N. P., Shrestha, B. K., Folasire, O., . . . Flo, T. H. (unbublished). Keap1 is recruited to mycbacterial phagosomes and regulates inflammatory signaling and autophagy in human macrophages.

Axe, E. L., Walker, S. A., Manifava, M., Chandra, P., Roderick, H. L., Habermann, A., . . . Ktistakis, N. T. (2010). Autophagosomeformation from membrane compartments enriched in phosphatidylinositol 3-phosphate and dynamically connected to the endoplasmic reticulum *Journal of Cell Biology, 182*, 17.

Ayabe, T., Satchell, D. P., Wilson, C. L., Parks, W. C., Selsted, M. E., & Ouellette, A. J. (2000). Secretion of microbicidal alpha-defensins by intestinal Paneth cells in response to bacteria. *Nature immunology, 1*, 6.

Barton, G. M., & Medzhitov, R. (2003). Toll-like receptor signaling pathways. *Science, 300*, 2.

Bjorkoy, G., Lamark, T., Brech, A., Outzen, H., Perander, M., Overvatn, A., . . . Johansen, T. (2005). p62/SQSTM1 forms protein aggregates degraded by autophagy and has a protective effect on huntingtin-induced cell death. *Journal of Cell Biology, 171*, 12.

Brennan, P. J. (2003). Structure, functions, and biogenesis of the cell wall of Mycobacterium tuberculosis. *Tuberculosis, 83*, 7.

Bryan, C. (2011). Infectious disease - Chapter 5: Mycobacterial diseases.

Bryan, H. K., Olayanju, A., Goldring, C. E., & Park, B. K. (2013). The Nrf2 cell defence pathway: Keap1-dependent and -independent mechanisms of regulation. *Biochemical Pharmacology, 85*, 13.

Bulut, Y., Michelsen, K. S., Hayrapetian, L., Naiki, Y., Spallek, R., Singh, M., & Arditi, M. (2005). *Mycobacterium tuberculosis* heat shock proteins use diverse Toll-like receptor pathways to activate pro-inflammatory signals. *The journal of biological chemistry, 280*, 7.

Cambi, A., & Figdor, C. G. (2003). Dual function of C-type lectin-like receptors in the immune system. *Current Opinion in Cell Biology, 15*, 8.

Castillo, E. F., Dekonenko, A., Arko-Mensah, J., Mandell, M. A., Dupont, N., Jiang, S., . . . Deretic, V. (2012). Autophagy protects against active tuberculosis by suppressing bacterial burden and inflammation. *Proc. Natl. Acad. Sci., 109*(9), 3168.

Catley, M. C., Chivers, J. E., & Cambridge, L. M. (2003). IL-1beta dependent activation of NF-kappaB mediates PGE2 release via the expression of cyclooxygenase-2 and microsomal prostaglansin E synthase. *FEBS letters, 547*, 5.

WHO report, (2013). Tuberculosis.

Clément, J.-F., Bibeaau-Poirier, A., Gravel, S.-P., Grandvaux, N., Bronneil, E. r., Thibault, P., . . . Servant, M. J. (2008). Phosphorylation of IRF-3 on Ser 339 generates a hyperactive form of IRF-3 through regulation of dimerization and CBP association. *Journal of virology, 82*, 13.

Davila, S., Hibberd, M. L., Hari Dass, R., Wong, H. E. E., Sahiratmadja, E., Bonnard, C., . . . Seielstad, M. (2008). Genetic association and expression studies indicate a role of Toll-like receptor 8 in pulmonary tuberculosis. *PLos Genetics, 4*, 8.

Davis, J. M., & Ramakrishnan, L. (2008). The role of the granuloma in expansion and dissemination of early Tuberculous infection. *Cell, 136*, 13.

de Koning, H. D., Simon, A., Zeeuwen, P. L. J. M., & Schalkwijk, J. (2012). Pattern recognition receptors in infectious skin diseases. *Microbes and Infection, 14*, 13.

Deretic, V. (2009). Multiple regulatory and effector roles of autophagy in immunity. *Current Opinion in Immunology, 21*, 10.

Deretic, V. (2012). Autophagy as an innate immunity paradigm: expanding the scpoe and repertoire of pattern recognition receptors. *Current Opinion in Immunology, 24*, 11.

Deretic, V., & Levine, B. (2009). Autophagy, immunity, and microbial adaptations. *Cell host and microbe, 5*, 22.

Dinkova-Kostova, A. T., Holtzclaw, W. D., & Kensler, T. W. (2005). The role of Keap1 in cellular protective responses. *Chemical Research in Toxicology, 18*, 13.

Dominska, M., & Dykxhoorn, D. M. (2010). Breaking down the barriers: siRNA delivery and endosome escape. *Journal of Cell Science, 123*, 7.

Elnifro, E. M., Ashshi, A. M., Cooper, R. J., & Klapper, P. E. (2000). Multiplex PCR: Optimization and application in diagnostic virology. *Clinical Microbiology Reviews, 13*, 12.

Fan, W., Tang, Z., Chen, D., Moughon, D., Ding, X., Chen, S., . . . Zhong, Q. (2010). Keap1 facilitates p62-mediated ubiquitin aggregate clearance via autophagy. *Autophagy, 6*, 8.

Farlik, M., Reutterer, B., Schindler, C., Greten, F., Vogl, C., Muller, M., & Becker, T. (2010). Nonconventional initiation complex assembly by STAT and NF-kappaB transcription factors regulate nitric oxide synthase expression. *Immunity, 33*, 10.

Flo, T. H., Smith, K. D., Sato, S., Rodriguez, D. J., Holmes, M. A., Strong, R. K., . . . Aderem, A. (2004). Lipocalin 2 mediates an innate immune response to bacterial infection by sequestrating iron. *Nature, 432*, 4.

Flynn, J. L., & Chan, J. (2001). Immunology of tuberculosis. *Annual review of Immunology, 19*, 37.

Franchi, L., Warner, N., Viani, K., & Nunez, G. (2008). Function of Nod-like receptors in microbial recognition and host defense. *Immunological reviews, 227*, 13.

Gandotra, S., Jang, S., Murray, P. J., Salgame, P., & Ehrt, S. (2007). Nucleotide-Binding Oligomerization Domain Protein 2-Deficient Mice Control Infection with *Mycobacterium tuberculosis*. *Infection and immunity, 75*, 8.

Geijtenbeek, T. B. H., & Gringhuis, S. I. (2009). Signalling through C-type lectin receptors: shaping immune responses. *Immunology, 9*, 15.

Geijtenbeek, T. B. H., Krooshoop, D. J. E. B., Bleijs, D. A., van Vliet, S. J., van Dujinhoven, G. C. F., Grabovsky, V., . . . van Kooyk, Y. (2000). DC-SIGN-ICAM-2 interaction mediates dendritic cell trafficking. *Nature immunology, 1*, 5.

Glick, D., Barth, S., & Macleod, K. F. (2010). Autophagy: cellular and molecular mechanisms. *The Journal of Pathology, 221*(1), 10.

Goldsby, R. A., Kindt, T. J., & Osborne, B. A. (2000). *Kuby Immunology*.

Halaas, O., Steigedal, M., Haug, M., Awuh, J. A., Ryan, L., Brech, A., . . . Flo, T. H. (2010). Intracellular Mycobacterium avium intersect transferrin in the Rab11+ recycling endocytic pathway and avoid Lipocalin 2 trafficking to the lysosomal pathway. *The Journal of Infectious Diseases, 201*, 10.

Hayden, M. S., & Ghosh, S. (2011). NF-kB in immunobiology (Review). *Cell reseach, 21*, 12.

Hayes, J. D., & McMahon, M. (2009). *Nrf2* and *Keap1* mutations: permanent activation of an adaptive response in cancer. *Trends in Biochemical sciences, 34*(4), 13.

Holmes, M. A., Paulsene, W., Jide, X., Ratledge, C., & Strong, R. K. (2005). Siderocalin (Lcn2) also binds carboxymycobactins, potentially defending against mycobacterial infections through iron sequestion. *Structure, 13*, 23.

Honda, K., & Taniguchi, T. (2006). IRFs: Mater regulators of signaling by Toll-like receptors and cytosolic pattern-recognition receptors. *Nature reviews immunology, 6*, 15.

Husebye, H., Aune, M. H., Stenvik, J., Samstad, E., Skjeldal, F., Halaas, O., . . . Espevik, T. (2010). The Rab11a GTPase controls Toll-like receptor 4-induced activation of interferon regulatory factor-3 on phagosomes. *Immunity, 33*, 14.

Ishii, K. J., Koyama, S., Nakagawa, A., Coban, C., & Akira, S. (2008). Host innate immune receptors and beyond: Making sense of microbial infections. *Cell host and microbe, 3*, 12.

Ishikawa, H., Ma, Z., & Barber, G. N. (2009). STING regulates intracellular DNS-mediated, type I interferon-dependent innate immunity. *Nature, 461*, 5.

Itoh, K., Wakabayashi, N., Katoh, Y., Ishii, T., Igarashi, K., Engel, J. D., & Yamamoto, M. (1999). Keap1 represses nuclear activation of antioxidant responsive elements by Nrf2 through binding to amino-terminal Neh2 domain. *Genes and Development, 13*, 11.

Jain, A., Lamark, T., Sjottem, E., Larsen, K. B., Awuh, J. A., Overvatn, A., . . . Johansen, T. (2010). p62/SQSTM1 is a Target Gene for Transcription Factor NRF2 and Creates a Positive Feedback Loop by Inducing Antioxidant Response Element-driven Gene Transcription. *The journal of biological chemistry, 285*, 16.

Jaiswal, A. K. (2010). Nrf2/INrf2 (Keap1) signaling in oxidative stress and cellular protection. 3.

Janssens, S., & Beyaert, R. (2003). Role of Toll-like receptors in pathogen recognition. *Clinical Microbiology Reviews, 16*, 10.

Jarlier, V., & Nikaido, H. (1994). Mycobacterial cell wall: Structure and role in natural resistance to antobiotics. *FEMS Microbiology Letters, 123*, 8.

Jin, Z., Li, Y., Pitti, R., Lawrence, D., Pham, V. C., Lill, J. R., & Ashkenazi, A. (2009). Cullin3-based polyubiquitination and p62-dependent aggregation of caspase-8 mediate extrinsic apoptosis signaling. *Cell, 137*, 15.

Kagan, J. C., Su, T., Horng, T., Chow, A., Akira, S., & Medzhitov, R. (2008). TRAM couples endocytosis of Toll-like receptor 4 to the induction of interferon-beta. *Nature immunology, 9*, 8.

Kaspar, J. W., Niture, S. K., & Jaiswal, A. K. (2009). Nrf2:INrf2 (Keap1) signaling in oxidative stress. *Free Radical Biology & Medicine, 47*, 6. doi: 10.1016/j.freeradbiomed.2009.07.035

Kawai, T., & Akira, S. (2006). TLR signaling. *Cell Death and Differentiation, 13*, 10.

Kawai, T., & Akira, S. (2009). The roles of TLRs, RLRs and NLRs in pathogen recognition. *International Immunology, 21*, 21.

Kawai, T., & Akira, S. (2011). Toll-like receptors and their crosstalk with other innate receptors in infection and immunity. *Immunity, 34*, 14.

Kim, J.-E., You, D.-J., Lee, C., Ahn, C., Seong, J. Y., & Hwang, J.-I. (2010). Suppression of NF-kB signaling by Keap1 regulation of IKKβ activity through autophagic degradation and inhibition of phosphorylation. *Cellular Signalling, 22*, 10.

Kiyoshi, T., & Shizuo, A. (2004). TLR signaling pathways. *Seminars in Immunology, 16*, 7.

Kleinnijenhuis, J., Oosting, M., Joosten, L. A. B., Netea, M. G., & Crevel, R. V. (2011). Innate immune recognition of *Mycobacterium tuberculosis*. *Clinical and Development Immunology*, 12.

Koirala, J. (2012). Medscape reference - Mycobacterium avium-intracellular.

Komatsu, M., Kurokawa, H., Waguri, S., Taguchi, K., Kobayashi, A., Ichimura, Y., . . . Yamamoto, M. (2010). The selective autophagy substrate p62 activates the stress responsive transcriptiom factor Nrf2 through inactivation of Keap1. *Nature Cell Biology, 12*, 11.

Kufer, T. A., Kremmer, E., Adam, A. C., Philpott, D. J., & Sansonetti, P. J. (2008). The pattern-recognition molecule Nod1 is localized at the plasma membrane at sites of bacterial interaction. *Cellular microbiology, 10*, 10.

Kumar, H., Kawai, T., & Akira, S. (2011). Pathogen recognition by the innate immune system. *International Reviews of Immunology, 30*, 19.

Lau, A., Wang, X.-J., Zhao, F., Villeneuve, N. F., Wu, T., Jiang, T., . . . Zhang, D. D. (2010). A noncanonical mechanism of Nrf2 activation by autophagy deficiency: direct interaction between Keap1 and p62. *Molecular and Cellular Biology, 30*, 11.

Lavelle, E. C., Murphy, C., O' Neill, L. A., & Creagh, E. M. (2009). The role of TLRs, NLRs, and RLRs in mucosal innate immunity and homeostasis. *Mucosal Immunology, 3*, 12.

Lee, D.-F., Kuo, H.-P., Liu, M., Chou, C.-K., Xia, W., Du, Y., . . . Hung, M.-C. (2009). Keap1 E3 ligase-mediated downregulation of NF-kB signaling by targeting IKKβ. *Molecular Cell, 36*, 10.

Levine, B., Sinha, S. C., & Kroemer, G. (2008). Bcl-2 family members: Dual regulators of apoptosis and sutophagy. *Autophagy, 4*, 7.

Liang, X. H., Kleeman, L. K., Jiang, H. H., Gordon, G., Goldman, J. E., Berry, G., . . . Levine, B. (1998). Protection against fatal Sindbis virus encephalitis by Beclin, a novel Bcl-2-interating protein. *Journal of virology, 72*, 11.

Manzanillo, P. S., Shiloh, M. U., Portnoy, D. A., & Cox, J. S. (2012). *Mycobacterium tuberculosis* activates the DNA-dependent cytosolic surveillance pathway within macrophages. *Cell host and microbe*, 12.

Martinon, F. (2010). Signaling by ROS drives inflammasome activation. *European Journal of Immunology, 40*, 4.

Mizushima, N. (2007). Autophagy: process and function. *Genes and Development, 21*, 13.

Moscat, J., & Diaz-Meco, M. T. (2006). Cell signaling and function organized by PB1 domain interactions. *Molecular Cell, 23*, 10.

Motohashi, H., & Yamamoto, M. (2004). Nrf2-Keap1 defines a physiologically important stress response mechanism. *TRENDS in Molecular Medicine, 10*, 9.

Niture, S. K., & Jaiswal, A. K. (2010). INrf2 (Keap1) targets Bcl-2 degradation and controls cellular apoptosis. *Cell Death and Differentiation, 18*, 13.

Ogura, T., Tong, K. I., Mio, K., Maruyama, Y., Kurokawa, H., Sato, C., & Yamamoto, M. (2010). Keap1 is a forked-stem dimer structure with two large spheres enclosing the intervention, double glycine repeat, and C-terminal domain. *Proceedings of the National Academy of Sciences of the United States of America, 107*, 6.

Pandey, A. K., Yang, Y., Jiang, Z., Fortune, S. M., Coulombe, F., Behr, M. A., . . . Kelliher, M. A. (2009). NOD2, RIP2 and IRF5 paly a critical role in the type I interferon response to *Mycobacterium tuberculosis*. *PLoS Pathog., 5*.

Pankiv, S., Clausen, T. H., Lamark, T., Brech, A., Bruun, J.-A., Outzen, H., . . . Johansen, T. (2007). p62/SGSTM1 binds directly to Atg8/LC3 to facilitate dagradation of ubiquitinated protein aggregates by autophagy. *The journal of biological chemistry, 282*, 15.

Pasparakis, M., Luedde, T., & Schmidt-Supprian, M. (2006). Dissection of the NF-kB signalling cascade in transgenic and knockdown mice. *Cell Death and Differentiation, 13*, 12.

Pathak, S., Awuh, J. A., Leversen, N. A., Flo, T. H., & Asjo, B. (2012). Counting Mycobacteria in infected human cells and mouse tissue: a comparison between qPCR and CFU. *PLoS ONE, 7*, 11.

Pattingre, S., & Levine, B. (2006). Bcl-2 inhibition of autophagy: A new route to cancer? *Cancer Research, 66*, 5.

Pattingre, S., Tassa, A., Qu, X., Garuti, R., Liang, X. H., Mizushima, N., . . . Levine, B. (2005). Bcl-2 antiapoptotic proteins inhibit Beclin 1-dependent autophagy. *Cell, 122*, 13.

Pedrosa, J., Flórido, M., Kunze, Z. M., Castro, A. G., Portaels, F., McFadden, J., . . . Appelberg, R. (1994). Characterization of the virulence of *Mycobacterium avium* complex (MAC) isolates in mice. *Clinical and Experimental Immunology, 98*, 7.

Pestka, S., Krause, C. D., & Walter, M. R. (2004). Interferons, interferon-like cytokines, and their receptors. *Immunological reviews, 202*, 25.

Pilli, M., Arko-Mensah, J., Ponpuak, M., Roberts, E., Master, S., Mandell, M. A., . . . Deretic, V. (2012). TBK1 promotes autophagy-mediated antimicrobial defense by controlling autophagosome maturation. *Immunity, 37*, 12.

Poligone, B., & Baldwin, A. S. (2001). Posotive and negative regulation of NF-kappaB ny COX-2: roles of different prostaglandins. *Journal of Biological Chemistry, 276*, 7.

Ramakrishnan, P., Wang, W., & Wallach, D. (2004). Receptor-specific signaling for both the alternative and the canonical NF-kappaB activation pathways by NF-kappaB-inducing kinase. *Immunity, 21*, 13.

Ratledge, C. (2004). Iron, mycobacteria and tuberculosis. *Tuberculosis (Edinb), 84*, 21.

Saunders, B. M., Dane, A., Briscoe, H., & Britton, W. J. (2002). Characterization of immune responses during infection with Mycobacterium avium strains 100, 101 and the recently sequenced 104. *Immunology and Cell biology, 80*, 6.

Schorey, J. S., & Cooper, A. M. (2003). Macrophage signalling upon mycobacterial infection: The MAP kinases lead the way. *Cellular microbiology, 5*, 10.

Seibenhener, M. L., Babu, J. R., Geetha, T., Wong, H. C., Krishna, N. R., & Wooten, M. W. (2004). Sequestosome 1/p62 is a polyubiquitin chain binding protein involved in ubiquitin proteasome degradation. *Molecular and Cellular Biology, 24*, 14.

Sherris Medical Microbiology. (2004). (K. J. Ryan & C. G. Ray Eds. 4th ed.): McGraw Hill.

Shi, Y., Chen, J., Weng, C., Chen, R., Zheng, Y., Chen, Q., & Tang, H. (2003). Identification of the protein-protein contact site and interaction mode of human VDAC1 with Bcl-2 family proteins. *Biochemical and Biophysical Research Communications, 305*, 8.

Simonsen, A., & Tooze, S. A. (2009). Coordination of membrane events during autophagy by multiple class III PI3–kinase complexes. *Journal of Cell Biology, 186*, 10.

Stepkowski, T. M., & Kruszewski, M. K. (2011). Molecular cross-talk between the Nrf2/Keap1 signaling pathway, autophagy, and apoptosis. *Free Radical Biology & Medicine, 50*, 10.

Sykiotis, G. P., & Bohmann, D. (2008). Keap1/Nrf2 signaling regulates oxidative stress tolerance and lifespan in Drosophila. *Cell Press, 14*, 10.

Takaoka, A., Wang, Z., Choi, M. K., Yanai, H., Negishi, H., Ban, T., . . . Taniguchi, T. (2007). DAI (DLM 1/ZBP1) is cytosolic DNA sensor and an activator of innate immune responses. *Nature, 448*, 5.

Takeuchi, O., & Akira, S. (2010). Pattern recognition receptors and Inflammation. *Cell Press, 140*, 16.

Tamura, T., Yanai, H., Savitsky, D., & Taniguchi, T. (2008). The IRF family transription factors in immunity and oncogenesis. *Annual review of Immunology, 26*, 50.

Taniguchi, T., Ogasawara, K., Takaoka, A., & Tanaka, N. (2001). IRF family of transciption factors as regulators of host defense. *Annual review of Immunology, 19*, 23.

Thurston, T., Ryzhakov, G., Bloor, S., von Muhlinnen, N., & Randow, F. (2009). The TBK1 adaptor and autophagy receptor NDP52 restricts the proliferation of ubiquitin-coated bacteria. *Nature immunology, 10*, 7.

Tian, H., Zhang, B., Di, J., Jiang, G., Chen, F., Li, H., . . . Zheng, J. (2012). Keap1: One stone kills three birds Nrf2, IKKb and Bcl-2/Bcl-xL. *Cancer Letters, 325*, 9.

Tojima, Y., Fujimoto, A., Delhase, M., Chen, Y., Hatakeyama, S., Nakayama, K., . . . Nakanishi, M. (2000). NAK is an IkB kinase-activating kinase. *Nature, 404*, 5.

Torrelles, J. B., Ellis, D., Osborne, T., Hoefer, A., Orme, I. M., Chatterjee, D., . . . M., C. A. (2002). Characterization of virulence, colony morphotype and the glycopeptidolipid of *Mycobacterium avium* strain 104. *Tuberculosis, 82*, 8.

Tschopp, J., & Schroder, K. (2010). NLRP3 inflammasome activation: The convergence of multiple signalling pathways on ROS production? *Immunology, 10*, 6.

Viatour, P., Merville, M.-P., Bours, V., & Chariot, A. (2005). Phosphorylation of NF-kB and IkB proteins: implications in cancer and inflammation. *Trends in Biochemical sciences, 30*, 10.

Virgin, H. W., & Levine, B. (2009). Autophagy genes in immunity. *Nature immunology, 10*, 10.

Wakabayashi, N., Itoh, K., Wakabayashi, J., Motohashi, H., Noda, S., Takahashi, S., . . . Yamamoto, M. (2003). Keap1-null mutation leads to postanal lethality due to constitutive Nrf2 activation. *Nature Genetics, 35*, 8.

Watson, R. O., Manzanillo, P. S., & Cox, J. S. (2012). Extracellular M.tuberculosis DNS targets bacteria for autophagy by activating the host DNA-sensing pathway. *Cell, 150*, 13.

Williamson, T. P., Johnson, D. A., & Johnson, J. A. (2012). Activation of the Nrf2-ARE pathway by siRNA knockdown of Keap1 reduces oxidative stress and provides partial protection from MPTP-mediated neurotoxicity. *NeuroToxicology, 33*, 8. doi: 10.1016/j.neuro.2012.01.015

Wolinsky, E. (1992). Mycobacterial diseases other than tuberculosis. *Clinical Infectious Diseases, 15*, 11.

Wooten, M. W., Hu, X., Babu, J. R., Seibenhener, M. L., Geetha, T., Paine, M. G., & Wooten, M. C. (2006). Signaling, polyubiquitination, trafficking, and inclusion: Sequestosome 1/p62's role in neurodegenerative disease. *Journal of Biomedicine and Biotechnology, 2006*, 12.

Wu, H., Santoni-Rugiu, E., Ralfkiaer, E., Porse, B. T., Moser, C., Hoiby, N., . . . Cowland, J. B. (2010). Lipocalin 2 is protective against *E. coli* pneumonia. *Respiratory Research, 10*, 8.

Zhang, D. D., Lo, S.-C., Sun, Z., Habib, G. M., Lieberman, M. W., & Hannink, M. (2005). Ubiquitination of Keap1, a BTB-Kelch substrate adaptor protein for Cul3, target Keap1 for degradation by a proteasome-independent pathway. *The journal of biological chemistry, 280*, 9. doi: 10.1074/jbc.M501279200

Appendix 1: TLR-family members, their ligands and origin, and their distribution in human cells

Receptor	Ligands	Origin	Adaptor protein(s)	Distribution	
				Location	Cell types
TLR-1	Triacyl-lipopeptides Lipoprotein Soluble factors	Bacteria Mycobacteria *Neisseria meningitidis*, *Borrelia burgdorferi*	MyD88 TIRAP	Cell surface	Monocytes, Macrophages, DCs, B cells, T cells, NK cells, PMN, Non-immune cells (*)
TLR-2	Peptidoglycan Lipoproteins LPA Atypical lipopolysaccharide, HSP 60/70, Surfactant protein-A Zymosan (beta-glucan) GPI anchor	Gram (+) bacteria Bacteria and mycoplasmas Bacteria Host cells Fungi, yeast *Trypanosoma cruzi* Trypanosomes, borrelias, listeria, klebsiella, herpes simplex virus	MyD88 TIRAP	Cell surface	Monocytes, Macrophages, Myeloid DCs, MCs, PMN, Non-immune cells
TLR-3	Double-stranded RNA Poly(I:C) acid Endogenous mRNA	Viruses Synthetic ligand Host cells	TRIF	Endosome	DCs, Macrophages, MCs, NK cells, Non-immune cells
TLR-4	LPS Envelope protein F protein HSP 60/70/90, Hyaluronic acid fragments, Saturated/unsaturated fatty acids, Surfactant protein-A	Gram (-) bacteria MMTV Respiratory syncytial virus Host cells	TRAM and TRIF MyD88 TIRAP	Cell surface	Monocytes, Macrophages, Myeloid DCs, MCs, PMN, Non-immunce cells
TLR-5	Flagellin Discontinous 13-aa peptide	Bacteria Synthetic analogue	MyD88	Cell surface	Monocytes, Macrophages, T cells, DCs, PMN, Non-immune cells
TLR-6	Diacyl lipopeptides LPA, Peptidoglycan	Mycoplasmas Bacteria	MyD88 TIRAP	Cell surface	Monocytes, Macrophages. B cells, T cells, DCs, PMN, NK cells, Non-immune cells
TLR-7	Single-stranded RNA Imiquimod	Viruses Synthetic compound	MyD88	Emdosome	Monocytes, Macrophages, Plasmacytoid DCs, B cells
TLR-8	Single-stranded RNA Resquimod	Viruses Synthetic compound	MyD88	Emdosome	Monocytes, Macrophages, MCs, Myeloid DCs
TLR-9	Unmethylated (CpG) DNA Double-stranded DNA	Bacteria Viruses	MyD88	Endosome	Monocytes, Macrophages, Plasmacytoid DCs, B cells, Epithelial cells, Keratinocytes
TLR-10	Pili	Bacteria	MyD88	Cell surface	Monocytes, Macrophages, B cells, Plasmacytoid DCs

LPA: lipoteichoic acid, HSP: heat shock protein, GPI: glycosyl phosphatidylinositol, Poly(I:C) acid: polyriboinosinic polyribocytidylic acid, LPS: lypopolysaccharide, MMTV: mouse mammary tumor virus, DCs: dendritic cells, NK cells: natural killer cells, PMN: polymorphonuclear neutrophil, MCs: mast cells.

(*) Non-immune cells: fibroblasts, astrocytes, epithelial cells, keratinocytes.

Appendix 2: Buffers and solutions used in western-blot

Buffer	Stock solution	
Lysis buffer (2x)		for 100ml:
** keep in -20°c*	Glycerol 87%	23ml
** dilute 1:1 with fresh benzonase and*	NaF 0.5M	20ml
proteinase inhibitor cocktail solution	Tris/HCl (pH 8.0) 1M	10ml
before using	EDTA (pH 8.0) 0.2M	1ml
	EGTA 0.2M	1ml
	NaCl 5M	15,4ml
	Triton X-100 10%	20ml
	Na_3VO_4 0.2M	1ml
	Sodium Deoxychelat 10%	10ml
	MiliQ water	up to 100ml
Benzonase and proteinase inhibitor		for 5ml:
cocktail solution	Benzonase 0.25U/ml	1.3µl
** make before use*	Proteinase inhibitor cocktail	1 tablet
	MiliQ water	5ml
Tris bufferef saline – with Tween (TBS-T)		for 1000ml:
** stored at room temperature*	Tris (pH 7.5) 1M	9.9ml
	Tween-20	1ml
	NaCl 5M	19.8ml
	Deionised water	up to 100ml
Mild tripping buffer (pH 2.2)		for 100ml:
	Glycine	1.5g
	SDS	0.1g
	Tween-20	1ml
	Deionised water	up to 100ml

Appendix 3: Blocking reagents for different phospho-antibodies in western-blot

	Incubated Ab (molecular weight - kDa)	**BSA / BSA + milk / Milk, respectively** * BSA: 5% BSA in TBS-T ** BSA + milk: 50:50 of 5% BSA and 5% dried-milk in TBS-T *** Milk: 5% dried-milk in TBS-T	**Comments**
1	p-NFkB –p65 (65)	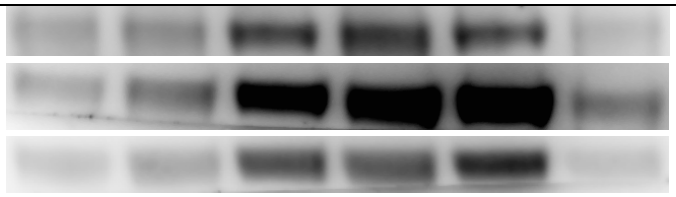	BSA + milk / milk > BSA (higher signal-to-noise & less background)
2	p-IKK gamma (50)	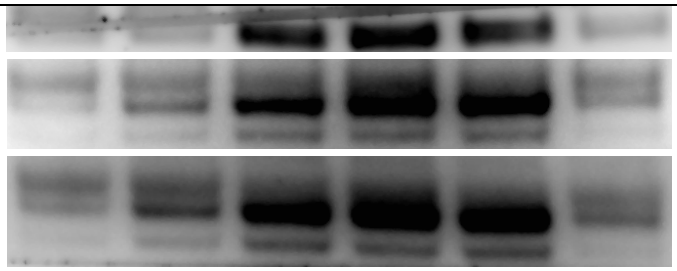	BSA > BSA + milk / milk (higher signal-to-noise)
3	p-p38 MAPK (43)	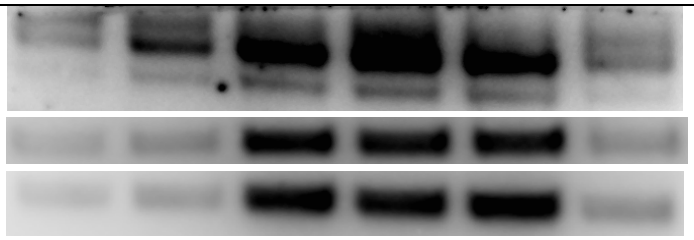	BSA + milk / milk > BSA (less background)
4	p-IKK alpha/beta (84-87)	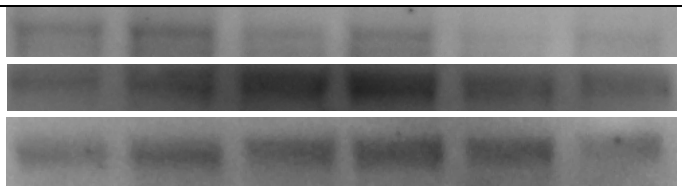	Hard to conclude
5	p-IRF3 (Ser396) (47)	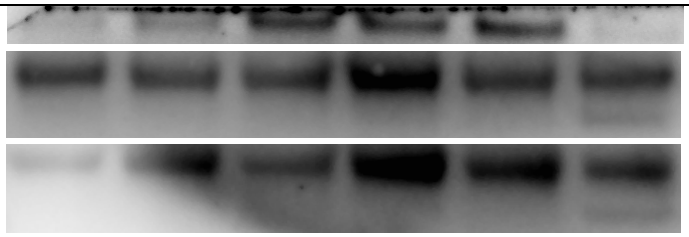	Worse than p-IRF3 (S386)
6	p-IKB (40)	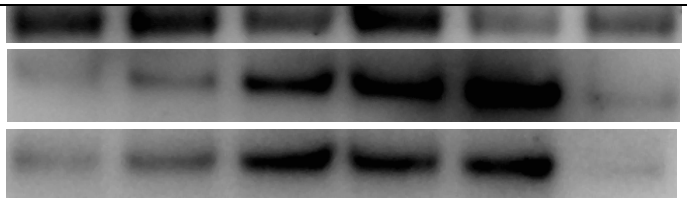	BSA > BSA + milk / milk (higher signal-to-noise, can observe control)

7	p-TBK1 (84)		BSA + milk / milk > BSA (more clear)
8	p-IRF3 (Ser386) (47)		BSA / BSA + milk > milk (more clear)
9	GAPDH (38)		Good with all reagents
MOI Mac infection (1 hour)		1:5 1:10 1:50 1:100 1:150 control *E.coli*	From MOI 1:50 to 1:150 gives clear results, not significant difference between them